7-2013

FABRICATION AND MODELING OF ELECTROCHEMICAL DOUBLE-LAYER CAPACITORS USING CARBON NANO-ONION ELECTRODE STRUCTURES

Fabio Parigi
University of Nebraska-Lincoln, fabioparigi@hotmail.com

FABRICATION AND MODELING OF ELECTROCHEMICAL DOUBLE-LAYER CAPACITORS USING CARBON NANO-ONION ELECTRODE STRUCTURES

by

Fabio Parigi

A DISSERTATION

Presented to the Faculty of

The Graduate College at the University of Nebraska

In Partial Fulfillment of Requirements

For the Degree of Doctor of Philosophy

Major: Electrical Engineering

Under the Supervision of Professor Jerry Hudgins

Lincoln, Nebraska

July, 2013

FABRICATION AND MODELING OF ELECTROCHEMICAL DOUBLE-LAYER CAPACITORS USING CARBON NANO-ONION ELECTRODE STRUCTURES

Fabio Parigi, Ph.D.

University of Nebraska, 2013

Advisor: Jerry Hudgins

Electrochemical capacitors or ultracapacitors (UCs) that are commercially available today overcome battery limitations in terms of charging time (from tens of minutes to seconds) and limited lifetime (from a few thousand cycles up to more than one million) but still lack specific energy and energy density (2-5% of a lithium ion battery). The latest innovations in carbon nanomaterials, such as carbon nanotubes as an active electrode material for UCs, can provide up to five times as much energy and deliver up to seven times more power than today's activated carbon electrodes. Further improvements in UC power density have been achieved by using state-of-the-art carbon nano-onions (CNOs) for ultracapacitor electrodes. CNO UCs could exhibit up to five times the power density of single-wall CNT UCs and could substantially contribute to reducing the size of an energy storage system as well as the volume and weight, thus improving device performance.

This dissertation describes the fabrication of CNO electrodes as part of an UC device, the measurement and analysis of the new electrode's performance as an energy storage component, and development of a new circuit model that accurately describes the CNO UC electrical behavior.

The novel model is based on the impedance spectra of CNO UCs and cyclic voltammetry measurements. Further, the model was validated using experimental data and simulation.

My original contributions are the fabrication process for reliable and repeatable electrode fabrication and the modeling of a carbon nano-onion ultracapacitor. The carbon nano-onion ultracapacitor model, composed of a resistor, an inductor, a capacitor (RLC), and a constant phase element (CPE), was developed along with a parameter extraction procedure for the benefit of other users. The new model developed, proved to be more accurate than previously reported UC models.

ACKNOWLEDGEMENT

I would like to extend my immense thanks to my advisor, Dr. Hudgins, and my doctoral committee members, Dr. Patterson, Dr. Lu, and Dr. Yoder, for the inspiring support and motivation during the intense and beautiful years I have spent at the University of Nebraska-Lincoln (UNL).

Also, I would like acknowledge my parents and my sister Lisa and her family for their unconditional love and support along this journey.

A special thank you should also be extended to my former advisor, Dr. Gandelli, who introduced me to the beauty of the high-level international carrier.

Among of all my friends and colleagues who supported me in different ways during this wonderful experience, I would like to give a special thanks to my girlfriend, Sara, Mauricio Casares, Dr. Gachovska, Pance Zaev, Dr. Martinez, Arindra Guha, Dr. Colton, Xu Yang, Daihyun Ha, Taesic Kim, Sue and Dr. Lipsky, David Bazinet and his family, Professor Coccimiglio, Professor Borzillo, Dr. Riedesel, Domenico Bee, Nathan Marsteller and Janina Krumbeck, Mark Bremer, Dr. Nasta, Elisa Carlini, Camilla Dell'Adami de Tarczal, Stefano Colombo, Dario Cataudella, Nithal Kuwa, Patrick Kazadi, Jose Herrero, Perica Tomic, Roberto Pilenga, Ben Jones, Ben Hornig, Dr. Gao, Dr. Zhou, Dr. Thirugnanam, Dr. Shah, Dr. Caňete, Thomas Smith, Joel Jacobs, Patricia Worster, Cheryl Wemhoff, Eva Bachman, the Latino and African communities, the Electrical Engineering department, and UNL.

TABLE OF CONTENTS

LIST OF FIGURES

LIST OF TABLES

SYMBOLS AND ABBREVIATIONS

A	Surface area of the electrode, m^2
AEC	Asymmetric electrolytic capacitor
β	Real exponent of the constant phase element
BET	Brunauer–Emmett–Teller area, m^2/g
C	Capacitance, F
C_2H_4	Ethylene
C_{dl}	Double layer capacitance, F
CNO	Carbon nano-onion
CNTs	Carbon nanotubes
CNT-a	Ionic-liquid-based gel electrolyte
CNT-b	Single-walled, organic gel electrolyte
CNT-c	Single-walled, aqueous gel electrolyte
CNT/PANI	Polyaniline-based electrodes
CNT/RuO_2	Single-walled carbon nanotube- Ruthenium(IV) oxide
CPE	Constant phase element
CSIRO	Commonwealth Scientific and industrial Research Organization
CV	Cyclic voltammetry
d	Double layer distance, m
D_c	Ion diffusion constant

DLC	Double layer capacitor
DoE	Department of Energy
E	Total energy, J
EC	Electrochemical capacitor
EIS	Electrochemical impedance spectroscopy
ε_0	Dielectric constant of free space, F/m
EPD	Electrophoretic deposition
EPR	Equivalent parallel resistance, Ω
ε_r	Relative permittivity
ESR	Equivalent series resistance, Ω
ESS	Energy storage system
F	Faraday's constant, C/mol
HEVs	Hybrid electric vehicles
i	Current, A
L	Inductor
L	Inductance, H
m	CNO weight, number of branches
MWCNT	Multi-walled carbon nanotubes
NCC	Nippon Chemi-Con Corporation
ND	Nano-diamonds

NEC	Nippon Electric Company
Ni	Plain Nickel
NiOOH	Positive electrode
P	Specific power, kW/kg
PSPICE	Personal simulation program with integrated circuit emphasis
PTFE	Tetrafluoroethylene
Q	Real constant
R	Series resistor, Ω
R_e	Internal resistance, Ω
R_c	Leakage resistance, Ω
SCESS	Supercapacitor energy storage system
SEM	Scanning electron microscope
SOHIO	Standard Oil of Ohio
SWCNT	Single-walled carbon nanotubes
UCs	Ultracapacitors
ΔV	Potential range, V
v	Voltage, V
V	Potential, V
V_1, V_2	Potential window voltage
W	Specific energy, Wh/k

ω	Angular frequency, rad/s
Z	Impedance, Ω
Z_p	Complex impedance, Ω
φ	Phase angle, °

CHAPTER 1. INTRODUCTION

The high cost of fossil fuel, national security concerns, and environmental awareness are driving efforts to find alternative solutions to the world's energy needs. Renewable energy is a possible solution to these issues, and advanced energy storage that not only matches its intrinsic variability but also improves energy system reliability and performance is required [1]. With the implementation of energy storage, the economics of the overall system are also affected, requiring, for example, a decrease in premium fuels and the related waste of energy [2]. Advances in fast energy storage for regenerative braking in hybrid electric vehicles (HEVs) could significantly increase their mileage range [3], or the load leveling made by water storage reservoirs in a hydropower generation plant could improve performance and efficiency, decreasing the total generation cost [2].

Energy can be stored in three main ways: mechanically, thermally, and electrochemically [2, 4].

A mechanical energy storage system includes: 1) a flywheel that uses the rotation of a mechanical device and its intrinsic moment of inertia to store rotational energy, 2) compressed air stored in underground reservoirs, extracted, heated, and expanded through a conventional gas turbine when needed [5], and 3) gravitational energy storage or pumped hydropower storage that utilizes the potential energy of the water to run turbines when needed.

Thermal energy can be stored: 1) as sensible heat, by increasing the temperature of a body, either liquid or solid; 2) as latent heat absorbed or released by a phase change

material when passing from one phase to another (gas, liquid, solid, or vice versa) and 3) by thermochemical reactions (energy transferred in the breaking and reforming of molecular bonds in a chemical reaction) [2].

Electrochemical energy storage includes either a Faradaic battery or non-Faradaic capacitor storage device. The classification of electrochemical energy storage [6-7] is depicted in Figure 1.1. (Chapter 3 provides more detail on electrochemical energy storage.)

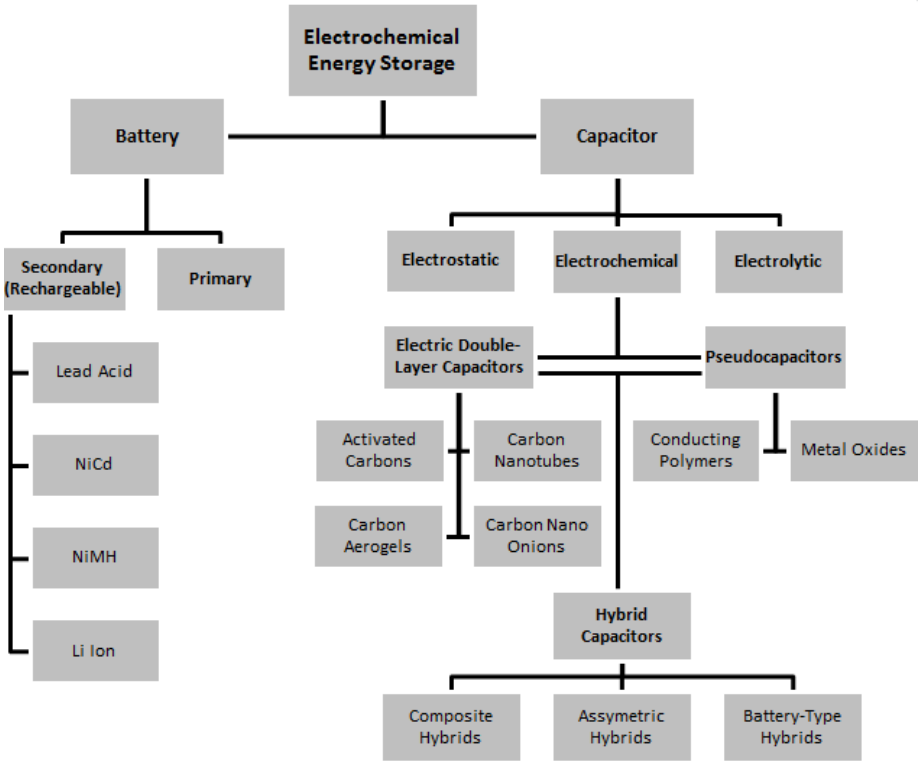

Figure 1.1. Classification of electrochemical energy storage.

The transportation sector is responsible for about 20% of the world's energy usage. Hence, safe, light, compact, and reliable energy storage capable of accommodating fast charging is required. Today's batteries require a long charging time (4-6 hours) and have a limited lifetime of up to a thousand cycles. This creates a

reliability problem. In addition, recycling is a challenge once the batteries reach the end of their lifetime [8].

To address some of these issues, research is currently focused on fast-charging, high-power, high-energy density, elevated charge-discharge cycle life energy storage for transportation applications [9]. Inside the electrochemical energy storage, batteries, especially lithium batteries, have been dominating the field of power sources and transportation [10].

Another family of electrochemical energy storage that has been receiving attention from researchers and industry is the electrochemical capacitor, also referred to as a double-layer capacitor or ultracapacitor (UC) due to its tremendous capacity density and almost unlimited charge-discharge cycle life [6, 11]. UCs have higher specific power than batteries and higher specific energy than regular capacitors [12]. A UC is an electrical energy storage apparatus that uses the ionic absorption at the interphase boundary between an electron conductor (e.g., aluminum foil) and an ionic conductor (e.g., ions in solution in electrolyte) by applying an electrostatic field across them [6].

For commercial UCs, it is common to find electrodes made of activated carbon [6, 13-14] and, most recently, carbon nanomaterials, such as carbon nanotubes [15]. An emerging nanomaterial for UC electrodes is the carbon nano-onion (CNO). CNOs provide high specific power, good energy density, and elevated cycling capability [16-18].

The objective of this research is to study the behavior of CNOs from an electrochemical point of view and to evaluate their applicability as an active material for

UC electrodes. Also, there is interest in developing an electrical equivalent circuit model for a CNO UC based on its impedance spectra and extending the previous work accomplished with activated carbon [6, 19-20] to CNOs. CNOs have been synthesized, and UCs made of CNOs have been assembled and characterized in the Nano-Engineering Laboratory at the University of Nebraska. Electrochemical measurements have been completed and an electric equivalent model developed. The simulation results match the experimental work precisely.

The development of an electric equivalent circuit model is important in providing engineers and designers with a new tool for studying advanced energy storage solutions for renewable energy applications, such as hybrid electric vehicles and consumer electronics.

1.1 Motivation of the Work

In the context of the theme introduced above, this dissertation is based on the modeling of a UC focusing on the (CNO).

The knowledge that it is possible to store energy in the interphase between a solid electrode and a liquid electrolyte dates back to the late 1800s [11]. It was only a few decades later, in 1957, that H.I. Becker of General Electric presented the first electric devices utilizing double-layer charge storage (Low Voltage Electrolytic Capacitor, U.S. Patent 2,800,616). Based on this discovery, R.A. Rightmire of Standard Oil of Ohio (SOHIO) invented, in 1962, the design that is commonly used today (Electrical Energy Storage Apparatus, U.S. Patent 3,288,641). This discovery opened a new era in energy storage devices dramatically increasing their energy-power density. Fig. 1.2 shows the

Ragone plot of the specific energy and specific power of the ultracapacitor energy storage devices.

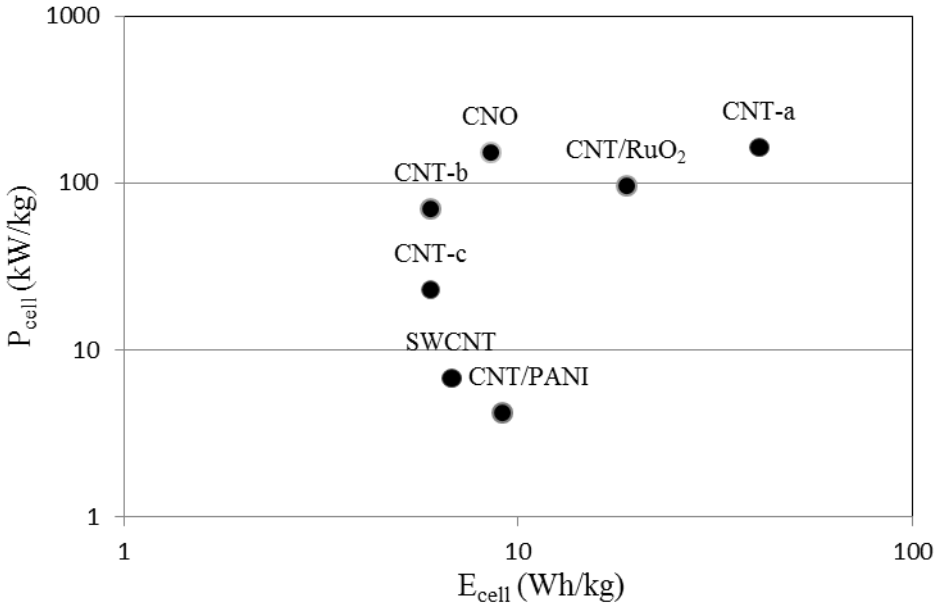

Figure. 1.2. Ragone plot. CNT-a: Ionic-liquid-based gel electrolyte [21]; CNT/RuO_2: single-walled [22]; CNT-b: Single-walled, organic gel electrolyte [23]; CNT-c: Single-walled, aqueous gel electrolyte [22]; SWCNT: Single-walled [22]; CNT/PANI: Polyaniline-based electrodes [24]; CNO: Carbon nano-onion [25].

It was almost 30 years later, in 1991, following advances in the research of high surface area materials, such as activated carbon, that the Japanese company, Nippon Electric Company, released the first activated carbon UC tremendously improving the capacity density of the device.

Formula 1 shows the dependence of the capacitance on the electrode's surface area, *A*, that is strictly related to the electrodes' material and the double layer distance, *d* (more details on the physics of a UC will be provided in the next chapter).

$$C = \varepsilon_0 \varepsilon_r \frac{A}{d} \quad (1)$$

The improvement in the device's capacitance affects its total energy as well, as presented in Formula 2.

$$E = \frac{1}{2} C V^2 \quad (2)$$

The key importance of electrode material in achieving high energy density devices is understandable.

A lot of research has been done to increase the surface area of electrodes (activated carbon reaches 760 m^2/g [115] and increase the power and energy density. However, the microporous structure of an activated carbon electrode is unfavorable for electrolyte wetting and rapid ionic motions, limiting power and energy density [15]. The introduction of CNTs as an active electrode material is an improvement. UCs made of CNTs can provide twice as much energy and deliver up to seven times more power than today's activated carbon electrodes [116].

Further improvements in power density have been achieved by using CNO material for ultracapacitor electrodes [16, 18]. The result is that CNOs exhibit up to five times the power density of single-wall CNTs [15]. Recent studies on the activation of CNOs [25] have shown an increment in the surface area of the material resulting in a little more exploration of the upper-right corner of the Ragone plot (Fig. 1.3). CNOs could substantially contribute to reducing the size of an energy storage system as well as the volume and weight, thus improving device performance. The physical aspect of CNO material could have a positive effect on the performance of electric vehicles with CNO UCs by increasing mileage or reducing weight. The more accessible surface area of CNO

material could enable a UC to handle peak currents and thereby fast charge/discharge applications. This feature could dramatically reduce, for example, the time required to charge portable devices such as laptops and cameras. The short charging time of UCs inspired us to design an advanced fast charger for an electric bicycle using CNO UCs for energy storage [26-27].

The potential uses highlight the need for computer simulation of CNO UCs which will extend the work achieved on activated carbon UCs to CNO UCs.

1.2 Research Accomplishments and Relevant Publications

The scientific contributions of this work are summarized as follows:

1. Characterization of a carbon nano-onion ultracapacitor
2. Modeling of a carbon nano-onion ultracapacitor
3. Development of a carbon nano-onion ultracapacitor application for electric bicycles

Publications associated with this dissertation are:

1. F. Parigi, J.L. Hudgins, Y.F. Lu, "Model of Electrochemical Double-Layer Capacitors Using Carbon Nano-Onion Electrode Structures." (Currently in submission process for *IEEE Transactions*.)
2. F. Parigi, T. Gachovska, Y. Gao, Y. Zhou, J.L. Hudgins and Y. Lu, "Carbon Nano-onions Ultracapacitor Model," *2013 MRS Materials Research Society Spring Meeting and Exhibit*, April 1-5, 2013, San Francisco, CA, USA.

3. F. Parigi, Y. Gao, T. Gachovska, J.L. Hudgins, D. Patterson, Y. Lu, ”Impedance-Based Simulation Model of Carbon Nano-Onions Ultracapacitors for e-Bike with Compact Energy Storage System,” *IEEE VPPC2012 Vehicle Power and Propulsion Conference*. 9-12 October 2012, Seoul, Korea.
4. F. Parigi, T. Gachovska, T. Kim, Y. Gao, D. Patterson, J.L. Hudgins, Y. Lu, “Minimal Energy Storage System Using Carbon Nanotube and Nano-Onion Ultracapacitors for an Electrified Bike,” *IASTED Power and Energy Systems, EuroPES 2012*, Jun 25-27, 2012, Naples, Italy.
5. F. Parigi, Y. Gao, M. Casares, T. Gachovska, Y.S. Zhou, Y.F. Lu, D. Patterson and J.L. Hudgins, “Investigations on the Aging Effect of Supercapacitors,” *2011 MRS Materials Research Society Spring Meeting and Exhibit*, April 25-29, 2011, S. Francisco, CA, USA.
6. F. Parigi, T. Gachovska, J. Hudgins, and D. Patterson, “Wind for Irrigation Application,” *IEEE Power Electronics and Machines in Wind Applications*, *PEMWA 2009*, June, 24-26, 2009, Lincoln, NE.

1.3 Literature Review

The literature review presented here covers different aspects of the UC world, including a brief history of UCs, materials, modeling, and applications.

1.3.1 History

Ultracapacitors are the result of an evolutionary process that began toward the end of the third quarter of the 19th century. In this section, we analyze the evolution of the

ultracapacitor's world from the dawn of the double layer phenomena through the latest carbon electrodes, such as activated carbon, carbon nanotubes, and carbon nano-onions, up to the awarding of the 2010 Nobel Prize in Physics to Andre Geim and Konstantin Novoselov for their work with graphene.

1861	G. Quincke introduced the concept of an electrical double layer [28], although he did not refer to it that way [29].
1874	The German physician and physicist H.V. Helmholtz, was the first to propose the model of the charge distribution around the boundary of a solid conductor and ions dissolved in a liquid. This intuition foresaw two opposite layers of charge, phasing each other at a few nanometers apart [30].
1909	L.G. Gouy and D. Chapman extended Helmoholtz's model by studying the thermal diffusion of ions and their diffusion distribution [31].
1924	O. Stern improved the Grouy-Chapman model by introducing a dimension of ions and solvent molecules, proposing that the charge was centered in the ion and placed at distance *d* from the solid plate and adding an absorbed ions zone near the electrode surface in

	conjunction with the Gouy-Chapman diffusion layer [31-32].
1947	D.C. Grahame proposed a comprehensive theory of the electrical double layer in a macro frame called electrocapillarity. Electrocapillarity studies the surface tension and an inert salt solution in contact with a metal. For Grahame, the double layer in a salt solution is an array of charges and dipoles between the solid and the ions. Also, he studied the double layer thermodynamic for different substances. He completed the Gouy-Chapman-Stern-Grahame theory, arriving at what is today known as the double layer model [29, 33].
1957	H.I. Becker of General Electric patented the first electrical device using double layer charge storage [34].
1962	R.A. Rightmire, of Standard Oil Company of Ohio (SOHIO) filed the patent and received it in 1966 for the device layout used today [35].
1969	SOHIO commercialized “Electrokinetic capacitor” energy storage for power rectification filtering based on high-surface-area carbon electrodes [11].

1970	D.L. Boos of SOHIO complemented Rightmire's patent on electrolytic capacitors having carbon paste electrodes [36] which became the technology cornerstone of modern electrolytic capacitors [11].
1972	Panasonic's Central Research Laboratory developed the first electric double layer capacitors (DLC), ideal for backup power and solar batteries [37].
1974	I.S. Lidorenko reported on a study, to the USSR Academy of Science, about a "molecular energy storage technology" that led to the development of kV-rated and MJ-rated capacitor systems for ignition of combustion engines [38].
1978	Panasonic of Kadoma, Osaka, Japan, began production of a DLC named "Golden Capacitors." The cell was composed of nonpasted electrode and nonaqueous electrolyte, rated at 1.8 V, and had two designs: one to replace the coin cell battery and a spiral-wound configuration [11].
	Nippon Electric Company (NEC), of Minato, Tokyo, Japan, commercialized SOHIO's Technology's first super-capacitor for backup power in volatile clock chips and consumer electronics. The novel design included the first

	bipolar configuration, aqueous electrolyte with pasted electrodes. The pasted electrode was made of conducting powder graphite and a binder [39]. Supercapacitor is NEC's registered trade name, so other names, such as ultracapacitor and double layer capacitor, should be used.
1980s	SOHIO began to produce a double layer capacitor with an aqueous electrolyte and dipolar configuration, rated several farads and 5.5 V, and labeled Maxcap® [11]. Maxcap technology was purchased by Carborundum and then by Cesiwid in 1993. Today it is referred to as Kanthal Globar [40].
1985	H.W. Kroto and colleagues from Rice University, Houston, Texas, observed a new stable carbon structure after vaporizing graphite by laser irradiation. It consisted of 60 carbon atoms placed on each vertex of a truncated icosahedron. It is an Archimedean solid, a polygon with 12 regular pentagonal faces, 20 regular hexagonal faces, with a total of 60 vertices and 90 edges (this shape is communally encountered in a soccer ball). Kroto named it C60: Buckminsterfullerene. Also, Kroto and colleagues observed that the C_{60} molecule had all valences satisfied by

	two single bonds and one double bond [41].
1987	ELNA America, Inc., patented an electric double layer capacitor, later commercialized as "Dynamocap," with organic electrolyte in coin cell and spiral-wound designs, for use in backup power supplies for IT, in sizes up to 200 F and 2.5 V, and a high power rate with an RC-time constant in the range of 0.1 to 1 sec [42].
1988	Electrochemical Power Sources (ELIT) of Kursk, Russia, produced the first asymmetric electrolytic capacitor (AEC), also referred to as "Hybrid Combined," which used two different electrodes and two electrochemical processes. The negative electrode, activated carbon, used the double layer to store the energy. The positive electrode, NiOOH, used a Faradaic process. Both electrodes were immersed in KOH electrolyte. The main advantage of the AEC is the selection of the operation voltage for each electrode leading to asymmetric operation of the electrodes, where each electrode has its own process speed and their difference, therefore, dictates the limitation of the asymmetric electric operation. AECs are indicated as starters for internal combustion energy motors at low

	temperature operation, UPSs, load-leveling systems, and stabilizing the energy flow in a power grid. The technical parameters of an AEC system are: 20 kJ-600 kJ up to 1000 V [43-45].
1990	ELIT shifted to a symmetrical design with two activated carbon electrodes and KOH electrolyte. Thanks to the prismatic form, the modules reached voltages as high as 400-1500 V [11].
1991	NEC reported achieving high capacitance using activated carbon composite material [11].
	Maxwell Technology, of San Diego, CA, USA, began working with the U.S. Department of Energy (DoE) to develop a technology able to level the energy peaks in electric vehicle battery energy systems. The proposed electrode was a metal-carbon fiber composite with KOH electrolyte. Later, the electrolyte was changed to organic and the electrode material from Ni-C to Al-C cloth [11].
	ECOND Corporation commercialized a bipolar type of capacitor with a double electric layer cell stack, with aqueous electrolyte for transportation applications with a

	focus on the starting energy of internal combustion engines [46].
	S. Iijima, a scientist at Fundamental Research Laboratories of NEC Corporation, Japan, presented a study on a new type of finite carbon structure in the form of needle-like tubes, later referred to as carbon nanotubes (CNTs). Iijima was fascinated by the Kroto's C_{60} [41] fullerene discovery and graphitic carbon sheets. Using a similar setup for the synthesis of C_{60}, he reported the formation of CNTs on the negative electrode of the arc-discharge of the evaporation process. The needle-like tubes were comprised of 2 to 50 graphitic sheets with diameters from a few to a few tens of nanometers [47].
1993	The incorporation of ESMA and ELTON, a Russian joint stock company based in Troitsk, Moscow, Russia, created a team of experts on the production and distribution of asymmetric electrochemical capacitors for heavy duty use (power buses and trucks) chargeable in 12-15 minutes for 1 hour of service. The cells were rated for 3,000-100,000 F, with systems rated 20 kJ-30 MJ at 14-190 V, and 10 Wh/kg energy density. The cells formed by a series of

	connected capacitors are inherently balanced due to the flooded configuration. The cells also had high cycle life and high power performance. The flooded battery design brought additional advantages with respect to organic electrolytes, moisture control avoidance, hermetic packaging removal, and material purity issues [48].
1996	The Commonwealth Scientific and Industrial Research Organization (CSIRO), Clayton South, Victoria, Australia, in partnership with Plessey Ducon, developed a high-specific energy, 9 Wh/kg, spiral-wound capacitor with carbon electrodes, organic electrolyte, and 1 second time constant [11].
1997	Cap-XX Pty Ltd was formed from the joint venture of CSIRO and Plessy Ducon to develop the most powerful electrolytic capacitor on the market designed for mobile and wireless communication systems. It had a series of connected cells, was rated 4.5 V, with a capacitance of 0.12- 0.8 F with ESR less than 0.1 Ω. Its RC time constant was less than 20 milliseconds [11].
	The Nippon Chemi-Con Corporation (NCC), Osaki, Shinagawa-ku, Tokyo, Japan, developed spiral-wound and

	prismatic cells, rated 3000 F and 2.5 V. Their products were optimized for energy or power delivery, and they provided test data that cleared up the reliability of electrochemical capacitors over time. With its innovative design, NCC avoided the health and fire issues of organic electrolytes by using propylene carbonate in the electrolyte. Also, to avoid the gas issues that generate swelling caused by the reactions of impurities during normal, or over-temperature and over-voltage operation, NCC employed an innovative pressure-regulation valve in the package. NCC cells found application in seaport cranes. They were used for storing regenerative energy produced while unloading container ships and reusing it in the lifting section of the loading process. The study showed 40% energy savings using this capacitor in seaport cranes [11].
	C. Niu and colleagues reported on a new type of electrochemical capacitor (EC) with carbon nanotube electrodes [49]. The electrodes were made of catalytically grown carbon nanotubes [50] [51] with an average diameter of ≈ 80 Å. Niu and colleagues, while reporting a

	step-by-step procedure to produce the electrode sheet, achieved an open structure that was not comparable with activated carbon or carbon fiber. The researchers studied the EC's capacitance at different frequencies, reporting a 102 F/g and 49 F/g at 1 and 100 Hz, respectively, and a specific power of > 8000 W/Kg. The electrolyte used was H_2SO_4 (38 wt %) [49].
	Wong and colleagues focused their studies on the extraordinary mechanical properties of nanorods and nanotubes [52].Tans and colleagues studied the electrical properties of single-walled carbon nanotubes (SWNTs), proving that SWNTs act as genuine quantum wires at least from contact to contact (140 nm) [53].
1998	NEC proposed a thin type of activated carbon band electrode rolled in a spiral-wound design [54].
	NESSCAP, from Giheung-gu, Yongin-si, and Gyeonggi-do, a Korean spinoff of the Daewoo Group, developed an organic electrolyte EC in spiral-wound prismatic configuration, presenting efficiency in stacking modules, with cells rated at 5000 F at 2.7 V. The cells were designed for transportation and power quality control. Another

	innovative design was a pseudo-capacitance high-energy EC with applications in solar-powered illumination along roads or in garden lights [11].
1999	Panasonic presented the "UpCap" capacitor, rated 2000 F and 2.3 V, for transportation applications. This device presented a double seal packaging, designed to prevent moisture from getting into the cell [11].
	Ma and collegues reported on an EC with CNT electrodes [55]. They investigated the influence of different mixtures and the performance of CNTs and phenolic resin powder as binders. They also reported a capacitance density of 15 to 25 F/cm^3 in H_2SO_4 (38 wt. %) electrolyte.
2001	NEC brought innovation to the packaging, introducing the first spiral-wound element and a low-profile ultracapacitor [11].
	J. H. Chen and colleagues focused their work on the electrochemical characterization of CNTs in double-layer capacitors. The cell used 50 nm diameter CNTs directly grown on graphite foil. Measurement, carried out by cyclic voltammetry, showed the typical double layer behavior

	with a specific capacitance of 115.7 F/g at 100 mV/s scan rate in 1 M H_2SO_4 electrolyte [113].
2002	ELNA was the first to report an asymmetric electrochemical capacitor with carbonaceous electrodes using organic electrolyte and lithium salts. They reported 16 Wh/l energy density and 4.2 V operating voltage [56], [57].
	Maxwell Technology incorporated the Swiss "Montena Components" acquiring the knowledge to boost their device's performance. Soon, Maxwell replaced the electrodes with carbon-coated aluminum foil and shifted to a spiral-wound cylindrical design as well. Cell size ranged 5-3000 F rated 2.7 V [11], [58].
2003	K.S. Kenneth and colleagues presented a study on superhydrophobic behavior, at a microscopic level, of CNT forests, achieved by covering the forests with a thin film of poly (tetrafluoroethylene) (PTFE). Kenneth and colleagues grew nanotubes by a chemical vapor technique directly on substrate and functionalized them with PTFE coating [114].

2004	K.S. Novoselov and co-workers discovered what has come to be known as graphene or 2D graphite: a single layer of carbon atoms assembled into a benzene-ring structure [59]. This two-dimensional graphite is the building block of graphitic-carbon-based materials such as: 0D fullerenes, or carbon nano-onions, 1D nanotubes (a graphene sheet rolled up into a cylinder of a few nanometers in diameter), or 3D graphite [60]. Therefore, the authors noticed how the arrangement of the structure of the material (0D, 1D, 2D, or 3D) while having the same chemical structure, could lead to completely different properties [61].
2005	P.L. Taberna and colleagues [62] studied a new activated carbon-carbon nanotube film for ultracapacitor applications. The performance of the cell, assembled with organic electrolyte (NEt_4BF_4 1.5 M in acetonitrile), was compared to pure activated carbon electrodes. A 15 wt. % of CNTs showed the best compromise between power and energy, achieving a specific capacitance of 88 F/g and resistance of 0.6 $\Omega \cdot cm^2$. In further study, the authors achieved 90 F/cm capacitance stable for 10,000 cycles [63].

2007	ESMA and its U.S. partner (American Electric Power) presented the first low-cost energy grid storage system for night-day usage. The system, an asymmetric capacitor made of oxide/sulfuric acid/activated carbon, has an optimal five hour charge/discharge cycle. It is charged during low peaks of energy consumption during the night and discharged at high peaks during daytime. It works at relatively slow frequencies (cycling rate), exactly one/day, and is projected to complete approximately 4,000 cycles over its ten-year lifetime. It is well suited for electrochemical capacitors and could challenge a regular battery system. ESMA designed a prototype system to be able to deliver 1 MW for 5 hours. These results are very encouraging from a technological point of view; however, they still have to prove the economic feasibility of the large energy-grid storage systems [11,64-65].
2008	P.W. Ruch and colleagues [66] studied the properties of SWCNTs as electrode materials for ultracapacitors, as suggested by previous research [67-69]. To characterize the electrochemical behavior of SWCNT electrodes, they utilized cyclic voltammetry, in situ Raman spectroscopy,

	and in situ dilatometry and compared the results with activated carbon material. They found that SWCNT capacitance is comparable to activated carbon.
	M. D. Stoller et al. [70] presented the first graphene-based ultracapacitors. The ultracapacitor's design takes advantage of the high surface area, 2630 m^2/g, and of the graphene, a 1-atom thick carbon sheet. The reported capacitances in organic and aqueous electrolyte were 99 F/g and 135 F/g, respectively.
2009	R. Signorelli and colleagues presented a detailed study on CNT material for EC electrodes. The voltage and accessible surface area limitation of activated carbon electrodes were discussed, and previous measurements of CNT EC electrodes were published. Signorelli *et al*. proposed a new vertically aligned CNT grown on substrate and reported a seven times higher energy density than commercial activated carbon ECs [116].
2011	M.H. Ervin *et al*. [71] presented a discussion on the fabrication methods of SWCNT ultracapacitor electrodes. They proposed an optimum method for fabricating SWCNTs based on solution-based electrodes. They

	investigated the influence of the deposition method and solution preparation on the double-layer capacitance. This method, in contrast to the direct grown on a current collector is thermal and chemical stress free. They also found that the deposition method might affect the porosity of the electrode.
2013	M.F.L. De Volder *et al*. [72] presented a review of carbon nanotube applications. Today, carbon nanotubes exist in two main forms: single-walled (SWCNTs) and multi-walled (MWCNTs), ranging from 0.8 to 2 nm and 5 to 20 nm, respectively, and from 100 nm up to cm in length. MWCNTs have 1 TPa of elastic modulus and 100 GPa tensile strength. CNTs can be either metallic or semiconducting depending on the orientation of the graphene lattice. Most of the CNTs today are made by chemical vapor deposition; and they are utilized in thin films, composite materials, active material for energy storage electrodes, antifouling coatings, and electrostatic discharge shielding.

In summary, we can delineate historically over 150 years of breakthroughs in the research and development of electrochemical capacitors. The material presented covers the primary contributions to the field, omitting niche markets and minor technologies.

Modeling of Activated Carbon Ultracapacitors

A literature survey on ultracapacitors began in the Spring of 2010. This section covers some of the most helpful references in understanding double layer capacitors and the evolution of the modeling of that phenomena for different materials, such as activated carbon, carbon nanotubes, and carbon nano-onions. This literature review covers, among others, the research carried out by: Grahame [29,33], Beliakov [44-45], Iijima [47], Kroto [41], Conway [13], Miller [6,11,14,65,73-74], Zubieta [75-77], Buller [20,78-80], Nelms [19,81-83], and Spyker [84-89]. Some authors propose, with good approximation, electric models to describe the double layer capacitor behavior.

J.R. Miller and A.F. Burke (1994) [73] published a testing procedures manual for electric vehicle capacitors. The manual provides test methods for evaluating the performance of ultracapacitors used for load leveling in battery applications on electric vehicles. A technique commonly used in battery technology is used for the DC signal characterization and a potentiostat and software from the electrochemistry field is used for AC impedance testing.

Spyker and Nelms (1996) [85,90] proposed a simple ultracapacitor model to simulate a DC/DC converter between the capacitor bank and a constant load. The model is composed of equivalent series resistance (ESR) and capacitance (C) with an equivalent

parallel resistance (EPR) that models the leakage effect. Hence, it will only impact long-term performance. The authors also present a study [84] (1997) on the discharge performance of different capacitors in two electrolytes: aqueous and organic. The values of ESR and C are obtained under different current and voltage conditions. Also, they examine [86] (1997) the application of ultracapacitors for high power and high energy storage. ESR and C are calculated under peak current capability and different load conditions. A DC/DC converter is used to control the voltage gain to compensate for voltage droops. They claim that the simple model, ESR in series with C, despite its simplicity, is a close approximation to real performance. During the high current performance study they looked at the high frequency pulse and inductance evaluation on a single capacitor and a short circuit test on three capacitors. They reported high peak current (570 A) under short circuit conditions and suggest taking these values into consideration when designing a DC/DC converter [87].

In further work [81] (1999), the authors compare the classical equivalent circuit with a ladder network. In particular, they focus on the slow discharge and pulse load. The parameters are extracted from experimental measurements through AC impedance data analysis. The important results in the capacitance calculation are due to a change in the stored energy method that is used to calculate initial capacitance, discharge capacitance, and capacitance change as a function of voltage. They found that ESR does not vary with frequency. Also, they reported that the classical equivalent circuit predicts more accurately the voltage of the cell during slow discharge, where in pulse load both equivalent circuits demonstrate good accuracy in predicting voltage drops.

In (2000), [89] presented a study on how to optimize arrays of ultracapacitor banks under a constant load connected through a DC/DC converter. Methods of predicting the behavior of supercapacitors in time, and predicting the final current and voltage level, were presented. The study shows that using a higher rated converter to increase the output power reduces run time and effective specific energy. To avoid this issue, it is possible to add in parallel strings of supercapacitors. In (2000) [88], they presented a similar study on slow discharge applications in regard to ultracapacitors. The change in storage energy method is used to study capacitance at different levels: initial, discharge mode, and dependence on voltage.

A.W. Leedy and R.M. Nelms studied [91] (2002) the capacitor-hybrid source for pulsed load applications. They presented a steady-state analysis to minimize the voltage deviation of a parallel system of a battery and/or fuel cell with ultracapacitors. They inferred that a hybrid source is suitable for pulse mode application and that the voltage ripple is proportional to the ESR. In PSPICE, the Ladder and classical circuit are simulated and compared with experimental data. Experiments and simulations are done at different voltage and dc bias levels.

Leedy and Nelms noticed that impedance magnitude increases as frequency decreases below 0.1 Hz; and the phase angle presents a capacity behavior below 1 Hz, a resistivity behavior in the mid-frequency range, and a phase angle that tends to 90 degrees after 35 kHz due to the inductance of the test leads. They measured and simulated the ESR, C, and leakage current and compared them. DC bias levels do not much affect the phase angle and magnitude [82].

Nelms *et al*. (2001) [83] presented an updated version of the double layer capacitor model represented by a Debye polarization cell. This new concept takes into account the chemical reactions which occur inside the capacitor. To achieve this model, the AC impedance is measured; and a nonlinear least square fitting method is used. Results of a Debye cell are compared to a regular cell. Simulation results in PSPICE are also presented and compared with the experimental data.

R. Bonet and L. Zubieta (1997) [75-76] presented a capacitor model with voltage dependence, capacitance, and a "normalization" procedure to achieve the repeatability and comparability measurements. Internal charge redistribution affects terminal voltage even though no charge has exchanges at the capacitor terminals. The normalization process proposes to stabilize the charge in 24 hr. and keep the EC terminal voltage under 1% variation.

F. Belhachemi *et al.* (2000) [32] proposed a physical model of a power electric double-layer capacitor based on the physics that govern the charge storage, which utilizes a transmission line with voltage dependence distributed capacitance.

E. Karden *et al.* (2000) [91] used impedance spectroscopy to determine the model structure and the model parameters of batteries with a focus on impedance, nonlinearity, voltage drift, stability, and data reproducibility due to the history of the battery.

S. Buller *et al.* (2001) [78] applied electrochemical impedance spectroscopy (EIS) to studying the dynamic behavior of ultracapacitors. The energy efficiency and the voltage response were simulated using Matlab/Simulink. The experiments were done at different temperature and voltage levels, called state of charge (SOC), for a frequency

range from 6 kHz to 10 microHz. The ultracapacitor was represented by a combination of an inductor (L), a series resistor (R), and complex impedance (Zp) that is a sequence of N RC circuits. Zp has only two independent parameters (t, C).

E. Karden and colleagues in [93] (2002) applied the EIS to model the dynamic, nonlinear, nonstationary behavior of electrochemical power sources. A porous electrode theory is included in the study. Experimental data are presented with equivalent circuit models under different direct current conditions. The study considers a supercapacitor, a lead/acid battery under charging and discharging operation, and the same type of battery at overcharge conditions. The authors show that the model parameters are correlated with the charge transfer kinetics, double layer capacitance, and pore structures of the electrodes. An ultralow frequency in conjunction with a DC operating current is needed to characterize the battery behavior. Monitoring the ohmic resistance will provide feedback on the state of health and state of the battery's charge.. S. Buller *et al*. in [79] (2005) utilizes the EIS to find new equivalent circuit models for ultracapacitors and lithium ion batteries. The proposed nonlinear, lumped-element model satisfies the accuracy requirement to simulate energy storage devices. This model is suitable for hybrid storage devices too.

Y.Y. Yao and colleagues (2006) [94] studied an equivalent model of supercapacitor under different conditions. Their model calculates ESR and EPR; and they study the voltage sharing effect and the overvoltage protection in series configuration. Their study is focused on aircraft applications, so they reproduce the radioactive space environment (high energy proton, x radial, gamma radial) with Co60 radiation; and they

have observed that the performance of the double layer capacitors decreases 12% under radiation exposition.

V. Martynyuk *et al*. (2007) [95] studied the nonlinear behavior of the DLC in a wide frequency range from a theoretical point of view. They explain the dependence of the capacitance and ESR on frequency and voltage level. They calculate the real value of capacitance and resistance at different working currents and voltages. The authors created a mathematical model to calculate supercapacitor parameters without doing experimental analysis.

H. Wu and R. Dougal (2005) [96] describe a novel dynamic multiresolution model for ultracapacitors. The model, simulated in a virtual test bed, a simulation platform, is a multiorder RLC circuit that dynamically switches the different orders during simulation. The switching that controls the simulation order is governed by the model output derivative. The model is validated in the simulation of an electric vehicle system.

D.A. New (2000) [97] proposes a detailed procedure to parameterize extraction of a double layer capacitor model. The model under consideration is Zubieta's model presented in multiple works [75-77,80].

F. Rafik *et al*. [98] (2006) use electrochemical impedance spectroscopy (EIS) to characterize ultracapacitors and to study the influence of frequency on ESR and capacitance. They analyze the frequency spectrum from 1mHz to 1 kHz. The authors developed an electrical model made of 14 RLC elements with parameters extracted from

experimental data using EIS. Good accuracy of the model vs. the experimental results was reported at different frequency, temperature, and bias voltage.

J. Huang *et al*. [99] (2008) developed an interesting, complete model for nanoporous ultracapacitors considering diverse pore size, carbon material, and electrolyte. The model follows a heuristic theoretical approach taking into account the pore curvature and the pore sizes. The model covers different material, such as activated carbon and carbide-derived material, and works for different electrolytes, such as organic, aqueous, and ionic liquid electrolytes. Also the authors discuss the effects of the kinetic solvation and desolvation process. Even though this is a complete model for porous materials, matching successfully the endohedral ultracapacitors, it presents limitations for exohedral ultracapacitors, such as carbon nanotubes with diameters smaller than 100 nm.

N. Bertrand and colleagues (2010) [100] developed a UC model taking into account its nonlinear behavior for embedded applications. The model follows, at first, the porous electrode theory and then an approximation of the results. A group of differential equations with fractional derivatives represents a set of fractional linear systems. A global model is then obtained through integration, where for each operating voltages there is a set of equations that represents the behavior of the UC at that particular voltage level.

S.H. Kim (2011) [101] proposes a dynamic simulation of a model for UCs considering parameter variation and self-discharge. Self-discharge is modeled by a constant phase element (CPE). To be able to simulate the CPE model in PSPICE, the

authors present three equivalent RC circuits. They state that CPE effectively represents the dynamic characteristics and self-discharge of the UC.

V. Musolino and colleagues (2013) [102] presented a UC model for the whole frequency range, including redistribution and self-discharge, that is a combination of Buller's model [20] and Zubieta's model [77]. Also, the authors provide a simple procedure for extracting the parameters from the data sheet of the UC. The simplicity of this procedure presupposes the availability of a datasheet. So, what seems to be an advantage could, in fact, be a limitation in dealing with experimental ultracapacitors where no data are available.

Modeling of Carbon Nanotubes Ultracapacitor

G.M. Odegard and colleagues (2002) [103] presented a model of a structure's property relationship with the nanomaterials. This model links solid mechanics and computational chemistry by utilizing the equivalent continuum model instead of the discreet molecular structures. The model has been used to study two different situations: the bending rigidity of the graphene sheet and the determination of the effective continuum geometry. The thickness and the bending rigidity of the graphene sheet were also determined.

A. Naeemi and J.D. Meindl (2007) [104] presented a physical model for single and bundles of walled carbon nanotubes valid for all voltages and lengths. The authors based their work on the results accomplished by M.W. Bockrath (1999) [105] and P.J. Burke (2002) [106] on a transmission line model on single-walled carbon nanotubes. The

transmission line model works as well from 1D to 3D conductor wires with nanometer diameters according to S. Salahuddin *et al*. (2005) [107].

A. Orphanou *et al*. developed a model of a carbon nanotube ultracapacitor, using a molecular dynamics approach based on ions' motion in the electrolyte between the electrodes. The frequency-dependent impedance is computed by applying an AC voltage and recording the current that is a function of the electrolyte and nanotube distribution. Finally, the cyclic voltammetry and Nyquist plots are presented vs. the lumped-element equivalent circuit simulation; and they demonstrate a high agreement.

Application of Ultracapacitors

Supercapacitors are used as energy storage in many commercial and military applications. They can be found on hybrid electric-gas propulsion systems, in hybrid ultracapacitor/battery solar energy storage, wind turbine pitch control systems, and electric metro trains, etc. In this literature review a few examples of applications will be presented.

R.M. Schupbach and J.C. Balda (2003) [108] presented a paper on how to design a hybrid battery-supercapacitor energy storage system. An ESS, including supercapacitors, offers weight and volume reduction and a better $/kW than a sole battery system. ESS with ultracapacitors not only maintains the same vehicle power and energy performance but achieves a better acceleration and an improvement in fuel consumption.

J.M. Miller *et al*. (2005) [74] presents a comparative study on ultracapacitors and battery energy storage systems (ESS) in hybrid vehicles with two different configurations of electronic continuously variable transmission. The article shows the benefits that

supercapacitors bring to the ESS. Pulse load supercapacitors present better performance than batteries, because batteries suffer from internal heating; tough ultracapacitors are indicated for repetitive cycling at a high pulse rate.

F. Rafik *et al*. (2006) [109] focused their work on DLC for vehicle application. Their study considers temperature, voltage, and frequency variations. The dynamics of the ions in the electrolyte are affected by the frequency, through the frequency dependence. At low frequency, the ions have the time to access entirely the pores' depth which correspond to an increase in the capacitance and ESR. At low temperature, the DLC's ESR increase.

R.M. Schupbach *et al*. (2003) [110] presents a work on the design aspects of an energy storage system composed of a battery and DLC for vehicle power management. The methodology shows how to choose the right combination between the battery and DLC based on energy density, power density, weight, and costs. The authors list the main steps to designing an energy storage system: determine the load requirements, find out the rated power of the principal energy source, and size the energy storage system considering the limitations imposed by the main energy source and the transient necessity.

T. Wei *et al*. (2007) [111] presents a study on DLC for a Wind Turbine Pitch control system. According to the authors, DLC guarantees reliable fast blade pitch control. The paper shows a comparison study among different energy storage components in term of advantages and disadvantages for pitch control. In conclusion, the authors

conclude that DLC are indicated for this application due to their power density, long operation cycling, and wide temperature range.

M.E. Glavin and W.G. Hurley (2007) [77] present research on a hybrid system composed of a battery and DLC for solar energy storage. According to the authors, the batteries of a photovoltaic system represent the reliability and cost in lifetime issues. Using a DLC and battery extends the battery's lifetime and makes the overall system more reliable and efficient. In a hybrid configuration, the DLC takes care of the peak power of the load; a size reduction in terms of volume and weight of the previous battery system.

Li *et al*. (2008) [112] presented research on an application of DLC for an energy storage system for wind power generation. According to the authors, the wind power fluctuations that affect the power quality can be improved by using a supercapacitor energy storage system (SCESS). The proposed SCESS system helps to smooth the medium frequency wind power fluctuations and helps to maintain the terminal voltage of the turbine at 1pu.

Literature

[1] H. P. Garg, S. C. Mullick, and A. K. Bhargava, *Solar Thermal Energy Storage,* D. Reidel Publishing Co, 1985.

[2] A. Sharma, V. V. Tyagi, C. R. Chen, and D. Buddhi, "Review on Thermal Energy Storage with Phase Change Materials and Applications," *Renewable and Sustainable Energy Reviews,* vol. 13, 2009, pp. 318-345.

[3] E. Karden, S. Ploumen, B. Fricke, T. Miller, and K. Snyder, "Energy Storage Devices for Future Hybrid Electric Vehicles," *Journal of Power Sources,* vol. 168, 2007, pp. 2-11.

[4] N. V. Khartchenko, *Advanced Energy Systems,* Berlin: Institute of Energy Engineering & Technology University, 1997.

[5] R. B. Schainker and M. Nakhamkin, "Compressed-Air Energy Storage (CAES): Overview, Performance and Cost Data for 25 mw to 220 mw Plants," *IEEE Transactions on Power Apparatus and Systems,* vol. 104, no. 4, April 1985.

[6] J. Miller, "Ultracapacitor Applications," *Power and Energy Series,* vol. 59, 2011.

[7] M. S. Halper and J. C. Ellenbogen, "Supercapacitors: A Brief Overview," March 2006, MP 05W0000272, MITRE, McLean, Virginia.

[8] F. C. McMichael and K. C. Henderson, "Recycling Batteries," *IEEE Spectrum,* February 1998.

[9] M. M. Thackeray, C. Wolverton, and E. D. Isaacs, "Electrical Energy Storage for Transportation—Approaching the Limits of, and Going Beyond, Lithium-ion Batteries," *J. of Energy & Environmental Science*, 2012, 5, 7854.

[10] G. Nazri and G. Pistoia, *Lithium Batteries: Science and Technology,* Springer ISBN 1402076282, 2004.

[11] J. R. Miller, "A Brief History of Supercapacitors," *Battery + Energy Storage Technology*, October 2007, p. 61-78.

[12] H. L. Becker and V. Ferry, U. S. Patent No. 2,800,616, July 23, 1957.

[13] B. E. Conway, *Electrochemical Supercapacitors: Scientific Fundamentals and Technological Applications,* Springer, 1999.

[14] J. R. Miller and A. F. Burke, "Electrochemical Capacitors: Challenges and Opportunities for Real-world Applications," *Electrochem. Soc. Interface*, vol. 17, no. 1, 2008, pp. 53-57.

[15] H. Pan, J. Li, and Y. P. Feng, "Carbon Nanotubes for Supercapacitor," *Nanoscale Res Lett*, 2010.

[16] A. S. Rettenbacher, B. Elliott, J. S. Hudson, A. Amirkhanian, and L. Echegoyen, "Preparation and Functionalization of Multilayer Fullerenes (Carbon Nano-Onions)," *Chemistry-A European Journal*, vol. 12, no. 2, December 2005, pp. 376-387.

[17] D. Pech, M. Brunet, H. Durou, P. Huang, V. Mochalin, Y. Gogotsi, P. L. Taberna, and P. Simon, "Ultrahigh-Power Micrometre-Sized Supercapacitors Based on Onion-Like Carbon," *Nature Nanotechnology*, vol. 5, July 2010, pp. 651-654.

[18] Y. Gao, Y. S. Zhou, J. B. Park, H. Wang, X. N. He, H. F. Luo, L. Jiang, and Y. F. Lu, "Resonant Excitation of Precursor Molecules in Improving the Particle

Crystallinity, Growth Rate and Optical Limiting Performance of Carbon Nano-Onions," *Nanotechnology*, vol. 22, no. 16, March 2011.

[19] R. M. Nelms, D. R. Cahela, R. L. Newsom, and B. J. Tatarchuk, "A Comparison of Two Equivalent Circuits for Double-Layer Capacitors," *Proc. IEEE APEC*, vol. 2, Mar. 1999, pp. 692-698.

[20] S. Buller, E. Karden, D. Kok, and R. W. De Doncker, "Modeling the Dynamic Behavior of Supercapacitors Using Impedance Spectroscopy," *IEEE Trans. Ind. Appl*., vol. 38, no. 6, Nov. / Dec. 2002.

[21] Y. J. Kang, H. Chung, C. H. Han, and W. Kim, "All-Solid-State Flexible Supercapacitors Based on Papers Coated with Carbon Nanotubes and Ionic-Liquid-Based Gel Electrolytes," *Nanotechnology*, vol. 23, 2012.

[22] P. Chen, H. Chen, J. Qiu, and C. Zhou, "Inkjet Printing of Single-Walled Carbon Nanotube/RuO2 Nanowire Supercapacitors on Cloth Fabrics and Flexible Substrates," *Nano Research*, vol. 3, issue 8, August 2010, pp. 594-603.

[23] M. Kaempgen, C. K. Chan, J. Ma, Y. Cui, and G. Gruner, "Printable Thin Film Supercapacitors Using Single-Walled Carbon Nanotubes," *Nano Letters*, vol. 9, issue 5, 2009, pp. 1872–1876.

[24] C. Meng, C. Liu, L. Chen, C. Hu, and S. Fan, "Highly Flexible and All-Solid-State Paperlike Polymer Supercapacitors," *Nano Letters*, vol. 10, issue 10, 2010, pp. 4025–4031.

[25] Y. Gao, Y. S. Zhou, M. Qian, X. N. He, J. Redepenning, P. Goodman, H. M. Li, L. Jiang, and Y. F. Lu, "Chemical Activation of Carbon Nano-Onions for High-Rate Supercapacitor Electrodes," *Carbon*, vol. 51, January 2013, pp. 52–58.

[26] F. Parigi, T. Gachovska, T. Kim, Y. Gao, D. Patterson, J. L. Hudgins, and Y. Lu, "Minimal Energy Storage System Using Carbon Nanotube and Nano-Onion Ultracapacitors for an Electrified Bike," IASTED Int. conf. EuroPES, 2012, Naples, Italy.

[27] F. Parigi, Y. Gao, T. Gachovska, J. L. Hudgins, D. Patterson, and Y. Lu, "Impedance-Based Simulation Model of Carbon Nano-Onions Ultracapacitors for E-Bike With Compact Energy Storage System," Vehicle Power and Propulsion Conference (VPPC), *IEEE*, Seoul, South Korea, October 9-12, 2012, pp. 1107 - 1111.

[28] Quincke, "Motion of Solid Particles Suspended in Liquids When Under Influence of Electric Current," *Journal of the American Chemical Society*, vol. 23, 1861, pp. 113, 513.

[29] D. C. Grahame, "The Electrical Double Layer and the Theory of Electrocapillarity," *Chemical Reviews*, vol. 41, issue 3, December 1947, pp. 441–501.

[30] H. V. Helmholtz, *Popular Lectures on Scientific Subjects*, 1st and 2nd series, trans. from German, vol. 2, 1873–81.

[31] M. Paunovic and M. Schlesinger, *Fundamentals of Electrochemical Deposition*, 1998.

[32] F. Belhachemi, S. Rael, and B. Davat, "A Physical Based Model of Power Electric Double-Layer Supercapacitor," Industry Applications Conference, *Conference Record of the 2000 IEEE,* vol. 5, Date of Conference: 2000, pp. 3069 – 3076.

[33] D. C. Grahame, "Effects of Dielectric Saturation Upon the Diffuse Double Layer and the Free Energy of Hydration of Ions," *J. Chem. Phys.*, 1950, pp. 18, 903.

[34] H. Becker, "Low Voltage Electrolytic Capacitor," U.S. Patent 2,800,616, July 23, 1957.

[35] R. A. Rightmire, "Electrical Energy Storage Apparatus," U.S. Patent 3,288,641, November 29, 1966.

[36] D. L. Boos, "Electrolytic Capacitor Having Carbon Paste Electrodes," U. S. Patent 3,536,963, October 27, 1970.

[37] Panasonic Industrial Company, Gold Capacitors Technical Guide, GCTG_CAT_0505.

[38] I. S. Lidorenko, "Anomalous Electrical Capacity and Experimental Models for Hyperconductivity," *Dokl. Akad. Nauk SSSR*, vol. 216, No. 6, 1974.

[39] T. Grygar, F. Marken, U. Schroder, and F. Scholz, "Electrochemical Analysis of Solids: A Review," *Collect. Czech. Chem. Commun.*, vol. 67, 2002.

[40] Kanthal Globar, Maxcap® Double Layer Capacitors, Form M-2004A - 09/07.

[41] H. W. Kroto, J. R. Heath, S. C. O'Brien, R. F. Curl, and R. E. Smalley, "C60: Buckminsterfullerene," *Letters to Nature,* vol. 318, November 14, 1985, pp. 162-163.

[42] H. Aruga, K. Hiratsuka, T. Morimoto, and Y. Sanada, "Electric Double Layer Capacitor," U. S. Patent 4,725,927 A, February 16, 1988.

[43] S. Razoumov , S. Litvinenko , A. Beliakov , "Asymmetric electrochemical capacitor and method of making," U.S. Patent 6,222,723, April 2001.

[44] A. I. Beliakov and A. M. Brintsev, "Development and Application of Combined Capacitors: Double Electric Layer-Pseudocapacity," Presented to The 7th International Seminar on Double Layer Capacitors and Similar Energy Storage Devices, Dec. 8-11, 1997, Deerfield Beach, FL.

[45] A. I. Beliakov and A. M. Brintsev, "Power Performances of High Energy Density Capacitors on System Carbon/Nickel Oxide," Presented at The 9th International Seminar on Double Layer Capacitors and Similar Energy Storage Devices, Dec. 6-8, 1999, Deerfield Beach, FL.

[46] G. I. Emelianov, A. Gerasimov, V. A. Ilyin, and A. M. Ivanov, U. S. Patent No. 5420747 A October 12, 1992.

[47] S. Iijima, "Helical Microtubules of Graphitic Carbon," *Letters to Nature,* vol. 354, November 7, 1991, pp. 56-58.

[48] S. Razoumov, A. Klementov, S. Litvinenko, and A. Beliakov, "Asymmetric Electrochemical Capacitor and Method of Making," U. S. Patent 6,222,723 B1, April 24, 2001.

[49] N. Chunming, E. K. Sichel, R. Hoch, D. Moy, and T. Howard, "High Power Electrochemical Capacitors Based on Carbon Nanotube Electrodes," *Applied Physics Letters,* vol. 70, issue 11, 1997, pp. 1480–1482.

[50] H. G. Tennent, Hyper Catalysis International, Inc., U. S. Patent 4,663,230, 1987.

[51] C. E. Snyder, W. H. Mandeville, H. G. Tennent, L. K. Truesdale, and J. J. Barber, WO Patent Appl. 89/07163, 1989.

[52] E. W. Wong, P. E. Sheehan, and C. M. Lieber, "Nanobeam Mechanics: Elasticity, Strength and Toughness of Nanorods and Nanotubes," *Science*, vol. 277, 1997, pp. 1971-1975.

[53] S. J. Tans, M. H. Devoret, H. Dai, A. Thess, R. E. Smalley, L. J. Geerligs, and C. Dekker, "Individual Single-Wall Carbon Nanotubes as Quantum Wires," *Letters to Nature*, vol. 386, April 3, 1997, pp. 474 – 477.

[54] G. Harada, J. Kurihara, and K. Sakata, "Electric Double Layer Capacitor and Manufacturing Method for Same," EP 0867902 A3, May 15, 2002.

[55] R. M. Ma, J. Liang, B. Q. Wei, B. Zhang, C. L. Xu, and D. H. Wu, "Study of Electrochemical Capacitors Utilizing Carbon Nanotube Electrodes," *Journal of Power Sources*, vol. 84, 1999, pp. 126-129.

[56] T. Morimoto, M. Tsushima, and Y. Che, Mat. Res. Soc. Proc., 575, San Francisco, CA, 357, 2000.

[57] M. Tsushima, Y. Che, and T. Morimoto, *Meeting Abstracts of ECS*, San Francisco, CA, Abstract no. 270, 2001.

[58] Maxwell Technology datasheet, Document number: 1015370.3.

[59] K. S. Novoselov, A. K. Geim, S. V. Morozov, D. Jiang, Y. Zhang, S. V. Dubonos, I. V. Grigorieva, and A. A. Firsov, "Electric Field Effect in Atomically Thin Carbon Films," *Science*, vol. 306, 2004, pp. 666.

[60] A. K. Geim and K. S. Novoselov, "The Rise of Graphene," *Nature Materials*, vol. 6, March 2007.

[61] K. S. Novoselov, D. Jiang, F. Schedin, T. J. Booth, V. V. Khotkevich, S. V. Morozov, and A. K. Geim, "Two-Dimensional Atomic Crystals," *Proceedings of the National Academy of Sciences*, vol. 102, no. 30, July 26, 2005, pp. 10451–10453.

[62] P. L. Taberna, G. Chevallier, P. Simon, D. Plee, and T. Aubert, "Activated Carbon–Carbon Nanotube Composite Porous Film for Supercapacitor Applications," *ELSEVIER, Materials Research Bulletin*, vol. 41, 2006, pp. 478–484.

[63] C. Portet, P. L. Taberna, P. Simon, and E. Flahaut, "Influence of Carbon Nanotubes Addition on Carbon-Carbon Supercapacitor Performances in Organic Electrolyte," *J. of Power Sources*, vol. 139, 2005, pp. 371-378.

[64] S. Razoumov, A. Klementov, S. Litvinenko, and A. Beliakov, "Asymmetric Electrochemical Capacitor and Method of Making," U. S. Patent 6,222,723, April 24, 2001.

[65] J. R. Miller, "Electrochemical Capacitor Thermal Management Issues at High-rate Cycling," *Electrochimica Acta*, vol. 52, issue 4, December 1, 2006, pp. 1703–1708.

[66] P. W. Ruch, D. Cericola, S. H. Ng, A. Foelske, and R. Kotz, "Single Wall Carbon Nanotubes for Supercapacitors Studied by In Situ Raman Spectroscopy and In Situ Dilatometry," *Proceedings of the 18th International Seminar on Double*

Layer Capacitors and Hybrid Energy Storage Devices, Deerfield Beach, USA, December 8-10, 2008, pp. 80-90.

[67] Ch. Emmenegger, Ph. Mauron, P. Sudan, P. Wenger, V. Hermann, R. Gallay, and A. Züttel, "Investigation of Electrochemical Double-Layer (ECDL) Capacitors Electrodes Based on Carbon Nanotubes and Activated Carbon Materials," *Journal of Power Sources,* vol. 124, issue 1, October 1, 2003, pp. 321-329.

[68] R. Signorelli, J. Schindall, and J. Kassakian, *Proceedings of the 14th International Seminar on Double Layer Capacitors and Hybrid Energy Storage Devices,* Florida Educational Seminar, 2004, pp. 49-61.

[69] C. Y. Liu, A. J. Bard, F. Wudl, I. Weitz, and J. R. Heath, "Electrochemical Characterization of Films of Single-Walled Carbon Nanotubes and Their Possible Application in Supercapacitors," *Electrochemical and Solid-State Letters,* 1999, pp. 577-578.

[70] M. D. Stoller, S. Park, Y. Zhu, J. An, and R. S. Ruoff, "Graphene-Based Ultracapacitors," *Nano Letters,* vol. 8, no. 10, 2008, pp. 3498-3502.

[71] M. H. Ervin, B. S. Miller, and B. Hanrahan, "SWCNT Supercapacitor Electrode Fabrication Methods," Army Research Laboratory, ARL-TR-5438, February 2011.

[72] M. F. L. De Volder, S. H. Tawfick, R. H. Baughman, and A. J. Hart, "Carbon Nanotube Present and Future Commercial Applications," *Science,* vol. 339, February 1, 2013.

[73] J. R. Miller and A. Burke, *Electric Vehicle Capacitor Test Procedures Manual*, Idaho National Engineering Laboratory, US Department of Energy, DOE/ID-10491, October 1994.

[74] J. M. Miller, P. J. McCleer, M. Everett, and E. G. Strangas, "Ultracapacitor Plus Battery Energy Storage System Sizing Methodology for HEV Power Split Electronic CVT's," Industrial Electronics, ISIE 2005. *Proceedings of the IEEE International Symposium on Industrial Electronics 2005*, vol. 1, Date of Conference: June 20-23, 2005, pp. 317 – 324.

[75] R. Bonert and L. Zubieta, "Measurement Technique for the Evaluation of Double-Layer Power Capacitors," IEEE Industry Applications Society Annual Meeting, New Orleans, Louisiana, October 5-9, 1997.

[76] L. Zubieta and R. Bonert, "Characterization of Double-Layer Capacitors (DLCs) for Power Electronics Applications," IEEE Industry Applications Conference, 33rd IAS Annual Meeting, vol. 2, October 1998, pp. 1149-1154.

[77] L. Zubieta and R. Bonert, "Characterization of Double-Layer Capacitors for Power Electronics Applications," *IEEE Trans. Ind. Applicat*., vol. 36, Jan/Feb 2000, pp. 199-205.

[78] S. Buller, E. Karden, D. Kok, and R. W. De Doncker, "Modeling the Dynamic Behavior of Supercapacitors Using Impedance Spectroscopy," *IEEE Transactions on Industry Applications*, vol. 38, issue 6, Date of Publication: Nov/Dec 2002, pp. 1622 – 1626.

[79] S. Buller, M. Thele, R. W. De Doncker, and E. Karden, "Impedance-Based Simulation Models of Supercapacitors and Li-ion Batteries for Power Electronics Applications," *IEEE Transactions On Industry Applications*, vol. 41, no. 3, May/June 2005.

[80] L. Zubieta, "Characterization of Double-Layer Capacitors for Power Electronics Applications," M.A.Sc. thesis, Dep. Of Elect. and Comput. Eng., University of Toronto, Toronto, Ont., Canada, 1997.

[81] R. M. Nelms, D. R. Cahela, R. L. Newsom, and B. J. Tatarchuk, "A Comparison of Two Equivalent Circuits for Double-Layer Capacitors," *IEEE*, 1999.

[82] R. M. Nelms, D. R. Cahela, and B. J. Tatarchuk, "Modeling Double-Layer Capacitor Behavior Using Ladder Circuits," *IEEE Transactions on Aerospace and Electronic Systems*, vol. 39, no. 2, April 2003.

[83] R. M. Nelms, D. R. Cahela, and B. J. Tatarchuk, "Using a Debye Polarization Cell to Predict Double-Layer Capacitor Performance," *IEEE*, 2001.

[84] R. L. Spyker and R. M. Nelms, "Discharge Characteristics of High Energy Storage Double Layer Capacitors," Energy Conversion Engineering Conference, IECEC, *Proceedings of the 32nd Intersociety*, vol. 1, Date of Conference: July 27-August 1, 1997, pp. 292 - 296.

[85] R. L. Spyker and R. M. Nelms, "Double Layer Capacitor/DC-DC Converter System Applied to Constant Power Loads," Energy Conversion Engineering Conference, IECEC, *Proceedings of the 31st Intersociety*, vol. 1, Date of Conference: August 11-16, 1996.

[86] R. L. Spyker and R. M. Nelms, "Evaluation of Double Layer Capacitors Technologies for High Power and High Energy Storage Applications," *IEEE,* 1997.

[87] R. L. Spyker and R. M. Nelms, "High Current Performance of 470 F Double-Layer Capacitors," *IEEE,* 1997.

[88] R. L. Spyker and R. M. Nelms, "Classical Equivalent Circuit Parameters for a Double-Layer Capacitors," *IEEE Transactions on Aerospace and Electric Systems,* vol. 36, no. 3, July 2000.

[89] R. L. Spyker and R. M. Nelms, "Optimization of Double-Layer Capacitor Arrays," *IEEE Transaction on Industry Applications,* vol. 36, no. 1, January/February 2000.

[90] R. L. Spyker and R. M. Nelms, "Evaluation of Double Layer Capacitors for Power Electronic Applications," Applied Power Electronics Conference and Exposition, APEC, *Conference Proceedings 1996,* Eleventh Annual, vol. 2, Date of Conference: March 3-7, 1996, pp. 725 - 730.

[91] A. W. Leedy and R. M. Nelms, "Analysis of a Capacitor-Based Hybrid Source Used for Pulsed Load Applications," 37th Intersociety Energy Convention Engineering Conference (IECEC), 2002.

[92] E. Karden, S. Buller, and R. W. De Doncker, "A Method for Measurement and Interpretation of Impedance Spectra for Industrial Batteries," *Journal of Power Sources,* vol. 85, 2000, pp. 72-78.

[93] E. Karden, S. Buller, and R. W. De Doncker, “A Frequency-Domain Approach to Dynamic Modeling of Electrochemical Power Sources,” *Electrochemical Acta,* vol. 47, 2002, pp. 2347-2356.

[94] Y. Y. Yao, D. L. Zhang, and D. G. Xu, “A Study of Supercapacitor Parameters and Characteristics,” *Power Systems Technology,* PowerCon 2006, October 22-26, 2006, pp. 1 – 4.

[95] V. Martynyuk, D. Makaryshkin, and J. Boyko. "Frequency Domain Analysis for Electrochemical Supercapacitors." *Proceedings of the 15th IMEKO TC–4 International Symposium on Novelties in Electrical Measurement and Instrumentations.–Iasi*. Vol. 2. 2007.

[96] H. Wu and R. Dougal, “Dynamic Multi-Resolution Modeling of Power Super Capacitor,” *Proceedings of the 37th Annual North American Power Symposium*, Date of Conference: October 23-25, 2005, pp. 241 – 246.

[97] D. A. New, “Double Layer Capacitors: Automotive Applications and Modeling,” M.A.Sc. thesis, Dep. Of Elect. Eng. And Comput. Science, Massachusetts Institute of Technology, USA, 2004.

[98] F. Rafik, H. Gualous, R. Gallay, A. Crausaz, and A. Berthon, “Frequency, Thermal and Voltage Supercapacitor Characterization and Modeling,” *J. of Power Sources,* vol. 165, 2007, pp. 928-934.

[99] J. Huang, B. G. Sumpter, and V. Meunier, “A Universal Model for Nanoporous Carbon Supercapacitors Applicable to Diverse Pore Regions, Carbon Materials and Electrolytes,” *Chem. Eur. J.*, 2008, pp. 6614-6626.

[100] N. Bertrand, J. Sabatier, O. Briat, and J. M. Vinassa, "Embedded Fractional Nonlinear Supercapacitor Model and its Parametric Estimation Method," *IEEE Transactions of Industrial Electronics*, vol. 57, no. 12, December 2010.

[101] S. H. Kim, W. Choi, K. B. Lee, and S. Choi, "Advanced Dynamic Simulation of Supercapacitors Considering Parameter Variation and Self-Discharge," *IEEE Transaction on Power Electronics*, vol. 26, no. 11, November 2011.

[102] V. Musolino, L. Piegari, and E. Tironi, "New Full-Frequency-Range Supercapacitor Model with Easy Identification Procedure," *IEEE Transaction on Industrial Electronics*, vol. 60, no. 1, January 2013.

[103] G. M. Odegard, T. S. Gates, L. M. Nicholson, and K. E. Wise, "Equivalent Continuum Modeling of Nano-Structured Materials," *Composites Science and Technology*, vol. 62, 2002, pp. 1869-1880.

[104] A. Naeemi and J. D. Meindl, "Design and Performance Modeling for Single-Walled Carbon Nanotubes as Local, Semiglobal, and Global Interconnect in Gigascale Integrated Systems," *IEEE Transactions on Electron Devices*, vol. 54, no. 1, January 2007.

[105] M. W. Bockrath, "Carbon Nanotubes: Electrons in One Dimension," Ph.D. dissertation, Univ. California, Berkeley, 1999.

[106] P. J. Burke, "Luttinger Liquid Theory as a Model of the Gigahertz Electrical Properties of Carbon Nanotubes," *IEEE Trans. Nanotechnology*, vol. 1, no. 3, September 2002, pp. 129-144.

[107] S. Salahuddin, M. Lundstrom, and S. Datta, "Transport Effect on Signal Propagation in Quantum Wires," *IEEE Trans. Electron Devices*, vol. 52, no. 8, August 2005, pp. 1734-1741.

[108] R. M. Schupbach and J. C. Balda, *The Role of Ultracapacitors in an Energy Storage Unit for Vehicle Power Management*, Vehicular Technology Conference, VTC 2003, IEEE 58th, vol. 5, Date of Conference: 6-9 October 6-9, 2003, pp. 3236 – 3240.

[109] F. Rafik, H. Gualous, R. Gallay, A. Crausaz, and A. Berthon, "Supercapacitors Characterization for Hybrid Vehicle Applications," Power Electronics and Motion Control Conference, IPEMC 2006. CES/IEEE 5th International, vol. 3, Date of Conference: August 14-16, 2006, pp. 1 – 5.

[110] R. M. Schupbach, J. C. Balda, M. Zolot, and B. Kramer, "Design Methodology of a Combined Battery-Ultracapacitor Energy Storage Unit for Vehicle Power Management," Power Electronics Specialist Conference, PESC 2003, IEEE 34th Annual, vol. 1, Date of Conference: June 15-19, 2003, pp. 88 - 93.

[111] T. Wei, S. Wang, and Z. Qi, "Design of Supercapacitor Based Ride Through System for Wind Turbine Pitch Systems," *Proceedings of International Conference on Electrical Machines and Systems*, Seoul, South Korea, Oct 8-11, 2007.

[112] Xiao Li, Changsheng Hu, Changjin Liu, and Dehong Xu, "Modeling and Control of Aggregated Super-Capacitor Energy Storage System for Wind Power

Generation," *Industrial Electronics*, IECON 2008, 34th Annual Conference of IEEE, Date of Conference: November 10-13, 2008, pp. 3370 – 3375.

[113] J. H. Chen, W. Z. Li, D. Z. Wang, S. X. Yang, J. G. Wen, and Z. F. Ren, "Electrochemical characterization of carbon nanotubes as electrode in electrochemical double-layer capacitors," *Carbon*, vol. 40, 2002, pp. 1193–1197.

[114] K. K. S. Lau, J. Bico, K. B. K. Teo, M. Chhowalla, G. A. J. Amaratunga, W. I. Milne, G. H. McKinley, and K. K. Gleason, "Superhydrophobic Carbon Nanotube Forests," *Nano Letters*, 2003, Vol. 3, No. 12, pp. 1701-1705.

[115] M. Hahn, P. Ruch, O. Barbieri, A. Foelske, R. Kötz, and R. Gallay, "Activated Carbons for Supercapacitors: The Impact of Charge-Induced Strain on Life Time and Performance Issues."

[116] R. Signorelli, D. C. Ku, J. G. Kassakian, and J. E. Schindall, "Electrochemical Double-Layer Capacitors Using Carbon Nanotube Electrode Structures," *Proceedings of the IEEE*, vol. 97 , issue 11, 2009, pp. 1837 – 1847.

CHAPTER 2. PHYSICS OF AN ULTRACAPACITOR

Electrochemical energy storage devices accumulate energy in a chemical and/or electrostatic way. The former are referred to as a battery, which are divided into primary and secondary batteries (rechargeable) and made of different materials, such as lead-acid, NiCd, NiMH, Li-ion. The latter form of energy storage device is called a capacitor. These are in turn classified as electrostatic, electrolytic, and electrochemical capacitors [1-2].

An electrolytic capacitor is a capacitor with one electrode that is not a conducting metal, referred to as an electrolyte. The electrolyte has lower conductivity than metal, so it is used when metallic electrodes are not viable. During the current flow from the anode to the bath cathode through the electrolyte, a dielectric layer of insulating metal oxide is formed on and into the anode surface. Its dielectric strength is a function of the thickness of the oxide layer. The oxide thickness and the associated voltage increase proportionally to the current flow. The advantage of electrolytic capacitors is the high capacitance per unit volume and per unit cost. Their main disadvantages are the limited life cycle due to electrolyte degradation and high energy loss due to electrolyte resistivity and they are unidirectional. Electrolytic capacitors should not be confused with electrochemical capacitors, which are based on the electrical double layer capacitance.

A double-layer capacitor, also called an ultracapacitor, is a charge storage device that accumulates charge on the interface of the double-layer formed between an electrolyte and an electrode when electrical potential is applied between them. A UC can accumulate a much higher electric charge than a regular capacitor. A typical capacitor has a value ranging from micro-Farads to milli-Farads. A typical UC can reach 5000 F with

activated carbon electrode material. Therefore, UCs are energy storage devices that present high specific power, great energy density, and elevated cycling capability, providing an interesting tool for industrial and consumer electronics applications [1]. Figure 2.1 shows the schematic comparison of a conventional capacitor, a double layer capacitor (DLC), and an asymmetric or hybrid capacitor [3].

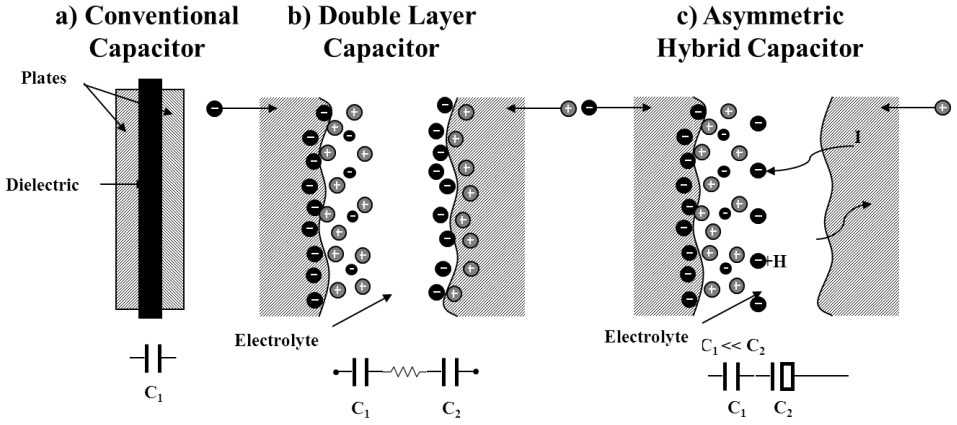

Figure 2.1. Schematic comparison of a: a) conventional capacitor, capacitance ranges from pF to µF; b) double layer capacitor, capacitance ranges from a few Farads to thousands of Farads, and c) asymmetric or hybrid capacitor, capacitance ranges from hundreds to thousands of Farads.

The UC is made of two electrodes sandwiching a separator that acts as an ionic conductor and electron insulator. The electrode is made of aluminum foil covered by activated powder carbon. The liquid electrolyte is between the electrodes and generally is made of various organic or aqueous solutions. When a voltage is applied to the electrodes, ions (anions and cations) start to migrate toward the electrode with the opposite polarity, creating two layers of opposite polarity near each phase boundary, hence the name double-layer capacitor. The capacitance, C is given by (2.1):

$$C = \varepsilon_0 \varepsilon_r \frac{A}{d} \tag{2.1}$$

where A is the electrode surface area, d the distance between the electrode and the layer of ions, ε_r is the relative static permittivity (sometimes referred to as the dielectric constant) of the material between the plates (for a vacuum, $\varepsilon_r = 1$), and ε_0 is the dielectric constant of free space ($\varepsilon_0 \approx 8.854 \times 10^{-12}$ F/m). Therefore, C is related to the electrodes' surface area and the double-layer distance d. For activated carbon, A could reach 2000 m^2/g, and d a few Å thick. Figure 2.2 illustrates a conceptual scheme of a double layer capacitor.

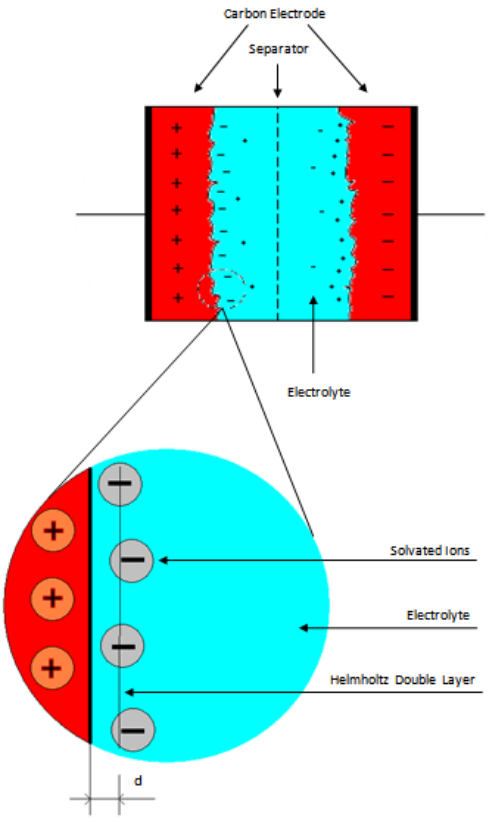

Figure 2.2. Double layer capacitor.

The latest research on fullerene materials has opened a new era of UC research and development. The tremendously high surface area of the fullerene family includes Buckminsterfullerene, also called buckyballs or C_{60} [4], and carbon nano-onions and carbon nanotubes . The CNT material is further characterized as being either single-walled (SWCNT) [5] or multiwalled (MWCNT) [6]. These carbon allotropes are ideal candidates for replacing the activated carbon of the current commercial UC electrodes. The CNT and CNO materials could dramatically increase UC energy and power density [5-7]. In Chapter 3, we will focus on carbon nano-onion material for UC electrodes.

The great potential for large-scale use of double layer capacitors as energy storage devices comes from the increased amount of energy that is stored at the border of the double layers due to the increased electric field (voltage) available. As shown in Eq. (2.2), the total energy stored in the capacitor is half of the product of the capacitance and the squared voltage. Another advantage of supercapacitors compared to batteries is that they can handle a large amount of current for a constant charging/discharging mode; the current can be on the order of ten times higher than the average rating for a limited amount of time (1 sec) [8]. Ultracapacitors provide interesting mechanical properties in terms of robustness and almost infinite cycle life [9]. Commercial companies guarantee that the maximum performance degradation in ten years stays below 20% [8].

$$E = \frac{1}{2}CV^2 \tag{2.2}$$

Compared to batteries, DLCs have higher specific power due to their ability to charge and discharge in a very small amount of time, due to low internal resistance and inductance. The main disadvantages of DLCs, when compared to batteries, are the lower

energy storage capability and lower voltage rate. The maximum voltage that a cell can reach is 3 V. This limit is due to impurities, and it is called the decomposition voltage. The double layer behaves as an insulator until the voltage reaches the break down level (3V) at which point current starts to flow [1].

LITERATURE

[1] B. E. Conway, "Electrochemical Supercapacitors: Scientific Fundamentals and Technological Applications," *Springer*, 1999.

[2] J. Miller, "Ultracapacitor Applications," *Power and Energy Series* 59, 2011.

[3] ELIT Joint Stock Corporation, "Electrochemical supercapacitors, technological and applications overview."

[4] H. W. Kroto, J. R. Heath, S. C. O'brien, R. F. Curl & R. E. Smalley, "C60: Buckminsterfullerene." *Letters to Nature* 318, 14 November 1985, pp. 162-163.

[5] K. H. An, W. S. Kim, Y. S. Park, J.-M. Moon, D. J. Bae, S. C. Lim, Y. S. Lee, Y. H. Lee, "Electrochemical Properties of High-Power Supercapacitors Using Single-Walled Carbon Nanotube Electrodes," *Advanced Functional Materials* vol. 11, issue 5, pages 387-392, October, 2001.

[6] C. Niu, E. K. Sichel, R. Hoch, D. Moy, H. Tennent, "High power electrochemical capacitors based on carbon nanotube electrodes," *Applied Physics Letters*,vol. 70, issue: 11, Mar 1997, pp. 1480-1482.

[7] Y. Gao, Y.S. Zhou, J.B. Park, H. Wang, X.N. He, H.F. Luo, L. Jiang, and Y.F. Lu, *Resonant excitation of precursor molecules in improving the particle crystallinity, growth rate and optical limiting performance of carbon nano-onions*, Nanotechnology, vol. 22, no. 16, Mar. 2011.

[8] Maxwell Technology datasheet, Document number: 1015370.3.

[9] F. V. Conte, F. Pirker, "Electrical Performance of High Power Electric Double Layer Capacitor under Thermal and Mechanical Stress."

CHAPTER 3. SYNTHESIS OF CARBON NANO-ONION

3.1 Chemistry of Carbon Nano-Onion

The work done by H.W. Kroto and co-workers in 1985 with laser desorption led to the creation of a new carbon allotrope, a cluster of 60 atoms named C60: Buckminsterfullerene [1-2]. W. Kratschmer *et al*. developed a large scale synthesis of CNO by electric arc discharge [3]. This method has been followed and, with small variations, utilized to synthetize other nanometric graphitic structures such as nanoparticles by Y. Saito and co-workers [4] and nanotubes by S. Iijima [5] and T. W. Ebbesen [6].

Transmission electron microscopy (TEM) has been a reliable technique used to study the structures of these carbon allotropes. D. Ugarte was the first to observe, using TEM, and label a carbon nano-onion, a nano-carbon spherical multilayered onion-like structure [7-8]. Fig. 3.1 is a TEM image of a CNO reproduced from reference [7].

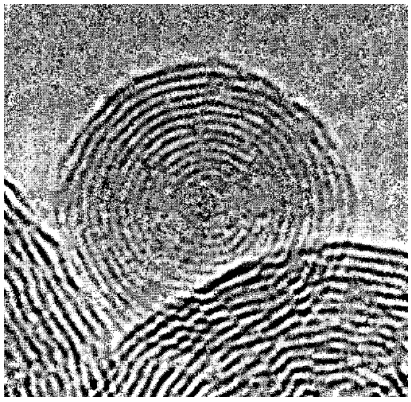

Figure. 3.1. Carbon nano-onion.

According to D. Ugarte, the concentric onion-like shells are about 0.334 nm from each other. This turns out to be the distance between two [220] graphitic plans [2]. Over

time, different synthesis techniques have been developed for CNO production. Kuznetsov *et al*. [10] synthetized CNOs by annealing 2-50 nm nanodiamonds (ND) at 800 °C. The ND annealing technique has a higher yield and lower cost than the electric arc technique as presented by W. Kratschmer *et al*. NDs, in the sp^3 diamond structure, are produced in bulk by detonation of RDX and TNT explosives in an inert environment [11].

In the literature, other different methods of synthesis of CNOs have been reported [12-21]. This chapter focuses on those which had a wider impact in the research field and presented a higher yield technique. Among them, we are focusing on nanodiamond annealing, arcing graphite underwater, and laser-assisted nanofabrication.

3.2 CNO Obtained from Annealing of NanoDiamond

The influence of temperature on nanodiamond production that lead to CNOs has been studied by different groups, including S. Tomita *et al*. [22], V.L. Kuzntsov [23], and E.D. Obraztova [24]. S. Tomita and co-workers found that annealing ND in a vacuum up to 800 °C does not affect the structure of the material. However, above that temperature, noncarbonaceous materials, which are eventually nested in it, began to register thermal desorption. The last noncarbon intruder, hydrogen, would leave the ND surface at approximately 850 °C [2,25-26]. E.D. Obraztsova *et al.* [24] observed a reduction of the surface energy of ND with an increase in the annealing temperature. Also, S. Tomita [22] suggests that upon higher annealing temperatures, the ND phase begins to change to a more graphitic phase. For temperatures above 900 °C, part of the external surface of the ND resists graphitization; but the core is still present as an ND structure. It is around 1100 °C where the smallest ND particles are completely transformed to a graphitic

structure, while the biggest particles have to reach approximately 1500 °C to complete the graphitic transformation. The result of the graphitization process is six or seven CNO shells. At temperatures between 1500-1800 °C the neighboring onions form joined graphitic layers. Moreover, the formation of multishell structures is observed at annealing temperatures above 2100 °C [2].

An interesting consequence regarding increases in the annealing temperature is the reduction of the equivalent internal resistance of electrodes from these materials, as reported by V.L. Kuznetsov [27]. He observed that up to the temperatures when the graphitization begins, the resistivity of the ND material is very high, on the order of 10^9 $\Omega \cdot cm^2$. After annealing the material at up to 1300 °C, the resistivity drops to 0.2-0.5 $\Omega \cdot cm^2$.

3.3 CNO Obtained From Arching Graphite Underwater

N. Sano *et al.* [27-28] presented a novel method to synthetize CNOs in a cheaper and simpler way than other methods, by performing arc discharges underwater. CNOs are 15-25 nm in diameter, have 20-30 shells, and are bigger compared to the 6-7 shells with 5 nm diameter of CNOs synthetized by annealing nanodiamond.

Two low-defect graphite rods were placed underwater. An arc was formed by applying a constant potential on the order of 16-17 V at 30 A. Then, CNOs were collected on the surface of the water, while other fullerenes, such as MWCNTs, were observed at the bottom of the pool. The floating state of the CNOs, despite their greater density than water, 1.64 g/cm^3, could be ascribed to the formation of large van der Walls crystals, as proposed by N. Sano [29].

CNOs produced by electric arc discharge give a Brunauer–Emmett–Teller (BET) surface area of 984.3 m^2/g, which it is greater than the reported values for CNTs [29]. The BET surface area is the measured area in m^2/g of the electrodes obtained by the BET theory [30]. The three scientists in 1938 discovered the relation between the adsorption of gas molecules on a solid surface and the material's specific surface area. Niu *et al.* reported a BET of 430 m^2/g for MWCNT [31], 357 m^2/g for SWCNT [32], where Futaba *et al.* presented a SWCNT-solid vertically aligned structure of 1000 m^2/g [33]. Raman spectroscopy has a 1450 cm^{-1} band known as the D band that can indicate the degree of disorder in graphene structures. Therefore, its absence implies perfect graphene structures. The spectroscopic 1582 cm^{-1} band of graphite is known as the G-band. One measure of the quality of graphene layers is to use the intensity ratio of D- and G-bands from the Raman spectroscopy [34]. The CNO material used in this work has measured D- (1344 cm^{-1}) and G-bands (1569-1577 cm^{-1}) from the Raman spectroscopy. Further discussion of the spectrum and comparison to other synthesis processes is given in [2,35]

Thanks to the properties of CNOs, many different applications have been reported, such as catalytic materials, lubricants, gas storage materials, ultracapacitors, optical limiters, and water purifiers [29,36-43].

An interesting note about CNOs is that their UV-visible characteristic is very close to the UV absorption spectrum of interstellar dust. As result, M. Chhowalla and co-workers [44] suggested that interstellar clouds may contain CNOs.

3.4 Laser-Assisted Nanofabrication of CNO

A.V. Kabashin and co-workers achieved, through a novel pulsed laser-assisted method, the fabrication of nanostructures [45]. Furthermore, this method has been used to grow CNTs [46-49]. Y.S. Zhou and co-workers [50] have also reported on their work with the laser-assisted nanofabrication of CNOs. The authors stated that exposing a material's surface to a laser has consequences, such as a narrow heating zone, melting, photochemical reactions, decompositions, etc. The irradiation of the surface of the material by photon beams at resonant excitation produces the breaking of these bonds and localized chemical reactions. Y. Gao and co-workers [51] proposed a methodology to produce, at a high growth rate (up to 2.1 g/hr), quality crystalline CNOs by exciting them with a 10.532 μm wavelength laser through ethylene (C_2H_4) molecules. The process was conducted in open air and used C_2H_4 and O_2 as precursors. A CO_2 laser beam at the 10.532 μm wavelength was directed into the flame generated by a welding torch. A silicon wafer was used to collect CNOs from the top of the flame. The G-band of the Raman spectra showed a crystallinity improvement when using the resonant excitation wavelength.

Literature

[1] H.W. Kroto, J. R. Heath, S. C. O'Brien, R. F. Curl & R. E. Smalley, "C60: Buckminsterfullerene." *Letters to Nature* 318, 162 – 163, 14 November, (1985).

[2] T. Akasaka, F. Wudl and S. Nagase. Chemistry of Nanocarbons. *John Wiley* & Sons Ltd (2010).

[3] W. Kratschmer, L. D. Lamb, K. Fostiropoulos and D. R. Huffman, Solid C_{60}: a new form of carbon. *Nature*, 347, 354-358 (1990). *Nature* **347**, 354 - 358 (27 September (1990); doi:10.1038/347354a0.

[4] Y. Saito, T. Yoshikawa, M. Inagaki, M. Tomita and T. Hayashi, "Growth and sctructure of graphitic tubule and polyhedral particles in arc-discharge." *Chem. Phys. Lett*., 204, 277-282 (1993).

[5] S. Iijima, *Helical microtubules of graphitic carbon*, *Nature* letter 354, 56 - 58 (07 November 1991); doi:10.1038/354056a0

[6] T. W. Ebbesen and P. M. Ajayan, "Large-scale synthesis of carbon nanotubes." *Nature*, 358, 220-222 (1992).

[7] D. Ugarte, "Onion-Like graphitic particles." Carbon, 33, 989-993 (1995).

[8] D. Ugarte, "Curling and closure of graphitic networks under electron-beam irradiation." *Nature*, 359, 707-709 (1992).

[9] E. Koudoumas, O. Kokkinaki, M. Konstantaki, S. Couris, S. Korovin, P. Detkov, V. Kuznetsov, S. Pimenov, and V. Pustovoi, "Onion-like carbon and diamond nanoparticles for optical limiting," *Chem. Phys. Lett*. 357, 336–340 (2002).

[10] V. L. Kuznetsov, A. L. Chuvilin, E. M. Moroz, V. N. Kolomiichuk, S. K. Shaikhutdinov, Y. V. Butenko and I. Y. Malkov, "Effect of explosion conditionson the structure of detonation soots – ultradisperse diamond and onio carbon." *Carbon*, 32, 873-882 (1994).

[11] V. L. Kuznetsov, A. L. Chuvilin, Y. V. Butenko, I. Y. Malkov and V. M Titov, "Onion –Like carbon from ultra-disperse diamond". *Chem. Phys. Lett*., 222, 343-348 (1994).

[12] A. Palkar, F. Melin, C. M. Cardona, B. Elliott, A. K. Naskar, D. D. Edie, A. Kumbhar, L. Echegoyen, "Reactivity Differences between Carbon Nano Onions (CNOs) Prepared by Different Methods." Chemistry – *An Asian Journal* Volume 2, Issue 5, pages 625–633, May 4, 2007.

[13] W. Lian, H. Song, X. Chen, L. Li, J. Huo, M. Zhao, G. Wang, "The transformation of acetylene black into onion-like hollow carbon nanoparticles at 1000 °C using an iron catalyst." *Carbon*, Volume 46, Issue 3, March 2008, Pages 525–530.

[14] L. C. Qin, S. Iijima, "Onion-like graphitic particles produced from diamond," *Chemical Physics Letters* Volume 262, Issues 3–4, 15 November 1996, Pages 252–258.

[15] V. V. Roddatis, V. L. Kuznetsov, Yu. V. Butenko, D. S. Su and R. Schlögl "Transformation of diamond nanoparticles into carbon onions under electron irradiation," *Phys. Chem. Chem. Phys*., 2002,4, 1964-1967.

[16] Gubarevich A.V.; Kitamura J.; Usuba S.; Yokoi H.; Kakudate Y.; Odawara O. "Onion-like carbon deposition by plasma spraying of nanodiamonds," *Carbon*, Volume 41, Number 13, 2003 , pp. 2601-2606(6).

[17] T. Gorelika, S. Urbanb, F. Falkb, U. Kaisera, U. Glatzela "Carbon onions produced by laser irradiation of amorphous silicon carbide," *Chemical Physics Letters* Volume 373, Issues 5–6, 28 May 2003, Pages 642–645.

[18] H. E. Troiani, A. Camacho-Bragado, V. Armendariz, J. L. G. Torresday, and M. J. Yacaman, "Synthesis of Carbon Onions by Gold Nanoparticles and Electron Irradiation," *Chem. Mater*., 2003, 15 (5), pp 1029–1031.

[19] Radhakrishnan, G.; Adams, P. M.; Bernstein, L. S. "Plasma characterization and room temperature growth of carbon nanotubes and nano-onions by excimer laser ablation," *Applied Surface Science*, Volume 253, Issue 19, p. 7651-7655.

[20] J. Hiraki, H. Mori, E. Taguchi, H. Yasuda, H. Kinoshita, and N. Ohmae, "Transformation of diamond nanoparticles into onion-like carbon by electron irradiation studied directly inside an ultrahigh-vacuum transmission electron microscope," *Appl. Phys. Lett*. 86, 223101 (2005).

[21] X.H Chen, F.M Deng, J.X Wang, H.S Yang, G.T Wu, X.B Zhang, J.C Peng, W.Z Li "New method of carbon onion growth by radio-frequency plasma-enhanced chemical vapor deposition,"

[22] S. Tomita, T. Sakurai, H. Ohta, M. Fujii, and S. Hayashi, "Structure and electronic properties of carbon onions," *J. Chem. Phys*. 114, 7477 (2001).

[23] Kuznetsov, V.L., Zilberberg, I.L. ; Butenko, Yu.V. ; Chuvilin, A.L. ; Segall, B. , "Theoretical study of the formation of closed curved graphite-like structures during annealing of diamond surface," *Journal of Applied Physics* (Volume:86 , Issue: 2) date of Publication: Jul 1999.

[24] E.D. Obraztsov, M. Fujii, S. Hayashi, V.L. Kuznetsov, Yu.V. Butenko, A.L. Chuvilin, "Raman identification of onion-like carbon," *Carbon* Volume 36, Issues 5–6, 1998, pp. 821–826.

[25] V. L. Kuznetsov, Y. V. Butenko, A. L. Chuvilin, A. Boronin, R. Kvon, S.V. Kosheev, "Self-assembled closed curved graphite-like structures (CCGS) formation on diamond surface," *Chemical Physics Letters* Volume 289, Issues 3–4, 12 June 1998, pp. 353–360.

[26] Y. V. Butenko, V. L. Kuznetsov, E. A. Paukshtis, A. I. Stadnichenko, I. N. Mazov, S. I. Moseenkov, A. I. Boronin and S. V. Kosheev, "The Thermal Stability of Nanodiamond Surface Groups and Onset of Nanodiamond Graphitization," *Fullerenes, Nanotubes and Carbon Nanostructures*, pp. 557-564 Volume 14, Issue 2-3, 2006.

[27] V.L. Kuznetsov, Y. V. Butenko, A.L. Chuvilin, A.I. Romanenko, A.V. Okotrub, "Electrical resistivity of graphitized ultra-disperse diamond and onion-like carbon," *Chemical Physics Letters* Volume 336, Issues 5–6, 23 March 2001, Pages 397–404.

[28] Sano N, Wang H, Chhowalla M, Alexandrou I, Amaratunga GA, "Synthesis of carbon 'onions' in water," *Nature*. 2001 Nov 29.

[29] N. Sano, H. Wang, I. Alexandrou, M. Chhowalla, K. B. K. Teo, G. A. J. Amaratunga, and K. Iimura, "Properties of carbon onions produced by an arc discharge in water," *J. Appl. Phys*. 92, 2783 (2002).

[30] S. Braunauer, P. H. Emmett, and E. Teller, "Adsorption of gases in multimolecular layers," *J. Amer. Chem. Soc*., vol. 60, no. 2, pp. 309–319 (1938).

[31] Niu, C., Sichel, E. K. ; Hoch, R. ; Moy, D. ; Tennent, H, "High power electrochemical capacitors based on carbon nanotube electrodes," *Applied Physics Letters*, Volume:70 , Issue: 11, Mar 1997 pp. 1480 – 1482.

[32] K. H. An, W. S. Kim, Y. S. Park, J.-M. Moon, D. J. Bae, S. C. Lim, Y. S. Lee, Y. H. Lee, "Electrochemical Properties of High-Power Supercapacitors Using Single-Walled Carbon Nanotube Electrodes," *Advanced Functional Materials* Volume 11, Issue 5, pages 387–392, October, 2001.

[33] D. N. Futaba, K. Hata, T. Yamada, T. Hiraoka, Y. Hayamizu, Y. Kakudate, O. Tanaike, H. Hatori, M. Yumura and S. Iijima, "Shape-engineerable and highly densely packed single-walled carbon nanotubes and their application as super-capacitor electrodes," *Nature Materials* 5, 987 - 994 (2006).

[34] J. Hodkiewicz, "Characterizing Carbon Materials with Raman Spectroscopy," *Thermo Fisher Scientific, Application Note*: 51901 (2010).

[35] Y. Gao, Y. S. Zhou, M. Qian, X. N. He, J. Redepenning, P. Goodman, H. M. Li, L. Jiang, and Y. F. Lu, "Chemical Activation of Carbon Nano-Onions for High-Rate Supercapacitor Electrodes," *Carbon*, vol. 51, January 2013, pp. 52–58.

[36] N. Keller, N. I. Maksimova, V. V. Roddatis, M. Schur, G. Mestl., Y. V. Butenko, V. L. Kuznetsov, R. Schlögl, "The Catalytic Use of Onion-Like Carbon Materials for Styrene Synthesis by Oxidative Dehydrogenation of Ethylbenzene," *Angewandte Chemie International Edition* Volume 41, Issue 11, pages 1885–1888, June 3, 2002.

[37] T. Cabioc'h, E. Thune, J. P. Rivière, S. Camelio, J. C. Girard, P. Guérin, M. Jaouen, L. Henrard, and Ph. Lambin, "Structure and properties of carbon onion layers deposited onto various substrates," *J. Appl. Phys*. 91, 1560 (2002).

[38] K.W. Street, M. Marchetti, R.L. Vander Wal, A.J. Tomasek, "Evaluation of the Tribological behavior of Nano-Onions in Krytox 143AB," *Tribology Letters* February 2004, Volume 16, Issue 1-2, pp 143-149.

[39] B. S. Xu, "Prospects and research progress in nano onion-like fullerenes," *New Carbon Mater*. 23, 289–301 (2008).

[40] C. Portet, G. Yushin, and Y. Gogotsi, "Electrochemical performance of carbon onions, nanodiamonds, carbon black and multiwalled nanotubes in electrical double layer capacitors," *Carbon* 45, 2511–2518 (2007).

[41] S. A. Maksimenko, V. N. Rodionova, G. Y. Slepyan, V. A. Karpovich, O. Shenderova, J. Walsh, V. L. Kuznetsov, I. N. Mazov, S. I. Moseenkov, A. V.

Okotrub, and P. Lambin, “Attenuation of electromagnetic waves in onion-like carbon composites,” *Diamond Relat. Mater.* 16, 1231–1235 (2007).

[42] X. W. Yang, J. J. Guo, X. M. Wang, X. G. Liu, and B. S. Xu, “Study on characterization and growth mechanism of Pt/onion-like fullerenes catalyst,” *Acta Phys.-Chim*. Sin. 22, 967–971 (2006).

[43] Y. L. Yao, X. M. Wang, J. J. Guo, X. W. Yang, and B. S. Xu, “Tribological property of onion-like fullerenes as lubricant additive*,” Mater. Lett*. 62, 2524–2527 (2008).

[44] M. Chhowalla, H. Wang, N. Sano, K. B. K. Teo, S. B. Lee, and G. A. J. Amaratunga, “Carbon Onions: Carriers of the 217.5 nm Interstellar Absorption Feature,” *Phys. Rev. Lett*. 90, 155504 (2003).

[45] A. V. Kabashin, P. Delaporte, A. Pereira, D. Grojo, R. Torres, T. Sarnet, and M. Sentis, “Nanofabrication with pulsed lasers,” *Nanoscale Res. Lett*. 5, 454–463 (2010).

[46] M. Mahjouri-Samani, Y. S. Zhou, W. Xiong, Y. Gao, M. Mitchell, L. Jiang, and Y. F. Lu, “Diameter modulation by fast temperature control in laser-assisted chemical vapor deposition of single-walled carbon nanotubes,” *Nanotechnology* 21, 395601 (2010).

[47] M. Mahjouri-Samani, Y. S. Zhou, W. Xiong, Y. Gao, M. Mitchell, and Y. F. Lu, “Laser induced selective removal of metallic carbon nanotubes,” *Nanotechnology* 20, 495202 (2009).

[48] Y. S. Zhou, W. Xiong, Y. Gao, M. Mahjouri-Samani, M. Mitchell, L. Jiang, and Y. F. Lu, "Towards carbon-nanotube integrated devices: optically controlled parallel integration of single-walled carbon nanotubes," *Nanotechnology*, 21, 315601,(2010).

[49] W. Xiong, Y. S. Zhou, M. Mahjouri-Samani, W. Q. Yang, K. J. Yi, X. N. He, S. H. Liou, and Y. F. Lu, "Self-aligned growth of single-walled carbon nanotubes using optical near-field effects," *Nanotechnology* 20, 025601 (2009).

[50] Y. S. Zhou, W. Xiong, J. Park, M. Qian, M. Mahjouri-Samani, Y. Gao, L. Jiang, and Y. Lu, "Laser-assisted nanofabrication of carbon nanostructures." *J. Laser Appl*. 24, 042007 (2012).

[51] Y. Gao, Y. S. Zhou, J. B. Park, H. Wang, X. N. He, H. F. Luo, L. Jiang, and Y. F. Lu, "Resonant excitation of precursor molecules in improving the particle crystallinity, growth rate and optical limiting performance of carbon nano-onions," *Nanotechnology* 22, 165604 (2011).

CHAPTER 4. CARBON NANO-ONION ULTRACAPACITOR

4.1 Electrophoretic Deposition

CNO material grown by a laser-assisted combustion process in open air was used for the study [1]. The CNO electrodes were fabricated by depositing CNOs on nickel (Ni) foam sheets using the electrophoretic deposition (EPD) technique. EPD has the following advantages: short formation time, simple apparatus, and suitability for mass production [2]. It has been successfully used for depositing uniform films in CNTs [3].

A solution containing 20 mg of CNO powder, 10 ml of acetone, and 10 ml of ethanol and 0.03-0.05 wt.% of aluminum nitrate nonahydrate $Al(NO)_3 \cdot 9H_2O$ was used for the EPD. The solution was placed in a 40 ml beaker and dispersed by sonication for 1 hour at room temperature (21 °C).

Two Ni foam sheets (thickness: 1.6 mm; surface density: 346 g/m^2; porosity: $\geq$ 95%, 80-110 pores per square inch, from Marketech International, Inc. U.S.) were washed in acetone by ultrasonication for 10 min. and dried for 24 hr. at room temperature. During the coating, one of the electrodes (10 x 10 mm) was used as the substrate and the other (20 x 20 mm) as a counter. The electrodes were placed in the solution, and a DC voltage was applied (80 V for 240 s). CNOs were deposited onto the anode. After that, the electrodes were dried at 80 °C for 24 hours. The weights of the electrodes before and after coating were recorded.

4.2 Electrochemical Measurements

A three-electrode system was used to examine the electrochemical performance of the ultracapacitor half-cell [4]. The system was composed of a Ni-CNO working electrode, an Ag/AgCl reference electrode, and a platinum wire for a pseudo-reference electrode; and it is shown in Fig. 4.1. The system was analyzed in 1 mol/l KNO_3 electrolyte and at room temperature. The impedance and cyclic voltammetry (CV) measurements were carried out using an electrochemical workstation (CH Instruments Model 760d, US).

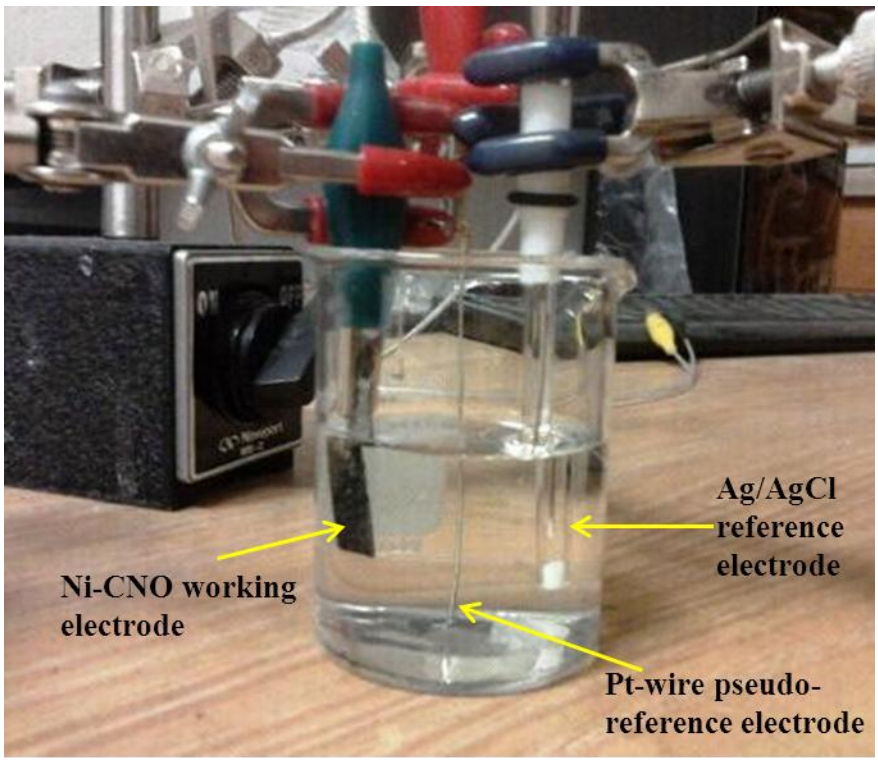

Figure 4.1. The three-electrode system used for the experiments.

The impedance between the working and reference electrodes was measured at 0 bias voltage with a sinusoidal signal amplitude of 1 mV and a frequency range of 10

mHz to 10 kHz. From the complex plane representation of measured impedance spectra, the equivalent series and the leakage resistance were found.

Cyclic voltammetry is a potentiodynamic electrochemical technique widely used for studying electrode processes [5]. A continuous cyclic potential is applied to a working electrode, and the working electrode current (i) vs. the applied potential (v) are recorded. The potential is linearly swept following a triangular waveform from the minimum (-0.4 V) to the maximum (0 V) potential at a scan rate of 50 mV/s, and then it is swept back while the current is recorded. The capacitance of the CNO is calculated from the CV curves. The results of these measurements are presented in Section 4.4.

4.3 Model

The proposed model for a CNO UC is a modified Randle's equivalent circuit. It consists of an inductor, L, an equivalent series resistance, R_e, a leakage resistance, R_c, a capacitance, C_{dl}, and a CPE.

A CPE is a circuit component that has a constant phase shift over a specified frequency band. CPEs have been used previously to model the dynamics of porous electrode structures made of activated carbon in UCs [6-8], the UC's self-discharge [9], and the CNO [10]. In this study, we are using the CPE to model the dynamic of the electrode structure of the carbon nano-onion UC. The CPE cannot be directly used in circuit simulation programs, such as MathWorks-Simulink™ or PSPICE™ [11]. Therefore, a procedure for converting a CPE into a lumped element passive RC network is used as a model [12]. Those parameters, in conjunction with the experimental data, were used as input values for ZView™ software (Version 3.3c). This program is often

used in electrochemical systems to minimize chi-squared and sum of square errors. The electric circuit model with the final parameters' values were then simulated using National Instrument's Multisim™ and compared with experimental data.

4.4 Measurements and Results

For this study, CNOs grown by the laser-assisted combustion synthesis process have been used [1]. The scanning electron microscope (SEM) images of the CNO electrode material are shown in Figure 4.2. The CNO diameter is in the range of 20 to 50 nm.

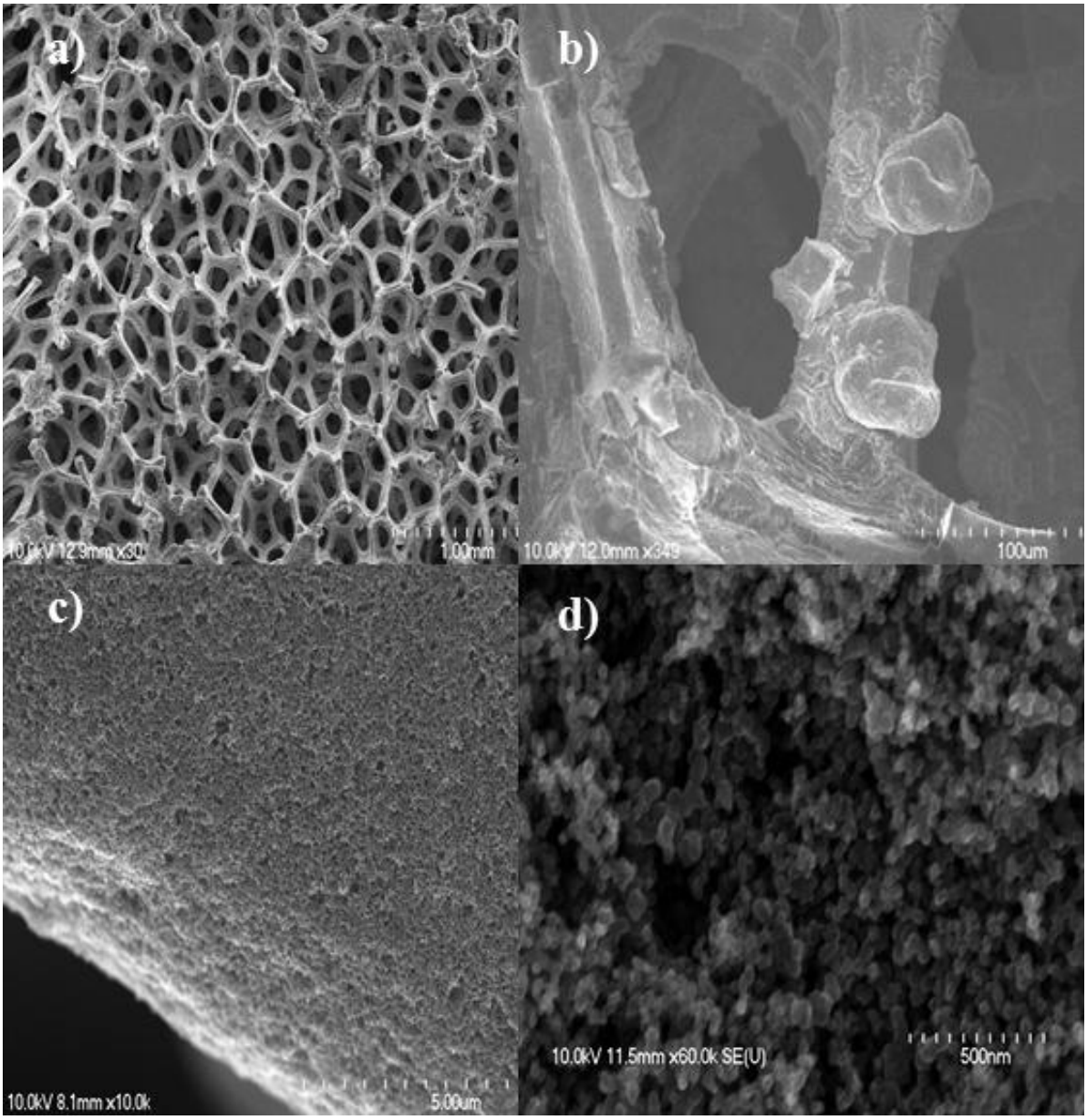

Figure 4.2. SEM images of: a) Plain Nickel (Ni) foam, scale 1 mm; b) Ni-foam with CNOs agglomerates, scale 100 µm; c) CNOs, scale 500 µm; d) CNOs scale 500 nm.

The electrochemical properties of CNOs were studied by electrochemical impedance spectroscopy and cyclic voltammetry in 1 mol/l KNO_3 electrolyte. The impedance spectra were investigated in the 10 mHz to 10 kHz frequency range. Fig. 4.3

shows the complex plane representation of the measured impedance spectra of a CNO UC obtained at 0 V dc bias and a sinusoidal signal amplitude of 1 mV; the inset shows its high frequency region. From the results presented in the inset of Fig. 4.3, it can be seen that the impedance spectra crosses the real axis at 1.96 Ω, known as internal resistance, R_e. It includes the ionic resistance related to the migration of electrolyte ions and resistance with the contacts. The frequency at which the impedance spectra cross the real axis, also called the resonant frequency, is 3.17 kHz. In addition, from Fig. 4.3, the leakage resistance, R_c, 2.27 Ω, is obtained by the intersection of the tangent of the impedance spectra at low frequency in the Nyquist plot with the real axis.

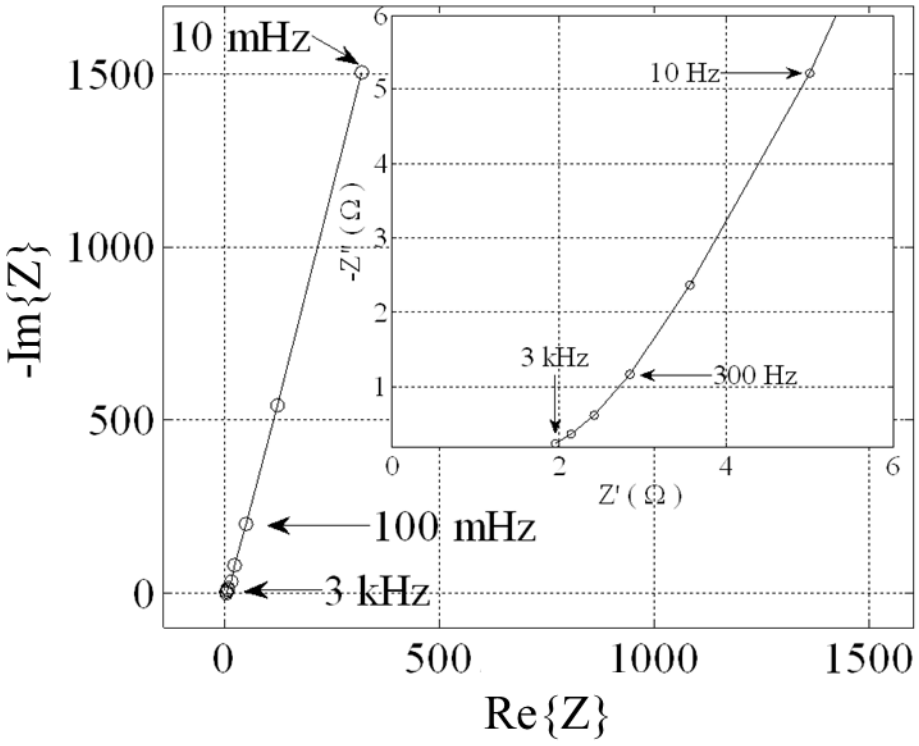

Figure 4.3. Complex plane representation of measured impedance spectra of a CNO UC obtained at 0 V dc bias and sinusoidal signal amplitude 1 mV over the frequency range of 10 mHz to 3 kHz. The results from 10 Hz to 3 kHz are shown in the inset.

Fig. 4.4a shows the CV curves of a CNO electrode measured at a 5 mV/s scan rate, for three different coating time conditions: 120 s, 240 s, and 480 s, all at 80 V. The current level increases with the coating time and reflects the CNO deposition rate.

All three coating times give a rectangular CV curve shape that indicates good overall CNO capacitance behavior. The CV measurements demonstrate stability; and particular redox reactions were not observed within the optimal potential window, from -400 mV to 0 mV. If redox reaction occurs, the CV curve will show spurious peaks that detract from the ideality of a capacitor. The optimum coating setup with the highest specific capacitance, 40 F/g, calculated using Eq. 4.1, is 120 s at 80 V/cm as can be observed in Fig. 4.4b. These values are used in this study. One reason why the capacitance is not linear with the coating time and drops off after 240 s is that it might depend on the peeling off of the CNO from the Ni-foam.

The capacitance, *C*, of the cell can be obtained by the integration of the voltammetric discharge from the cyclic voltammogram according to [13-14]:

$$C = \frac{\int i dV}{v m \Delta V} \tag{4.1}$$

where *i* is the charging current at steady state when applying a voltage *v* (sweep rate, mV/s); and *m* is the CNO weight and ΔV the potential range of the CV measurement.

The specific power, *P* (kW/kg), and specific energy, *W* (Wh/kg), defined as (4.2) and (4.3), respectively, can be calculated by the following equations [13,15]:

$$P = \int_{V_1}^{V_2} i \; dV \tag{4.2}$$

$$W = \frac{\Delta V}{v \, 3600} \int_{V_1}^{V_2} i \; dV \tag{4.3}$$

where i is the current, V is the potential, V_1 and V_2 are the voltages of the potential window of the CV presented in Fig. 4.4a, v is the scan rate (in mV/s), and ΔV is the discharge potential range (in V).

The CNO's specific W, P, and C are summarized in Table 1 in conjunction with some relevant literature regarding other carbon electrode materials, activated carbon, and CNTs.

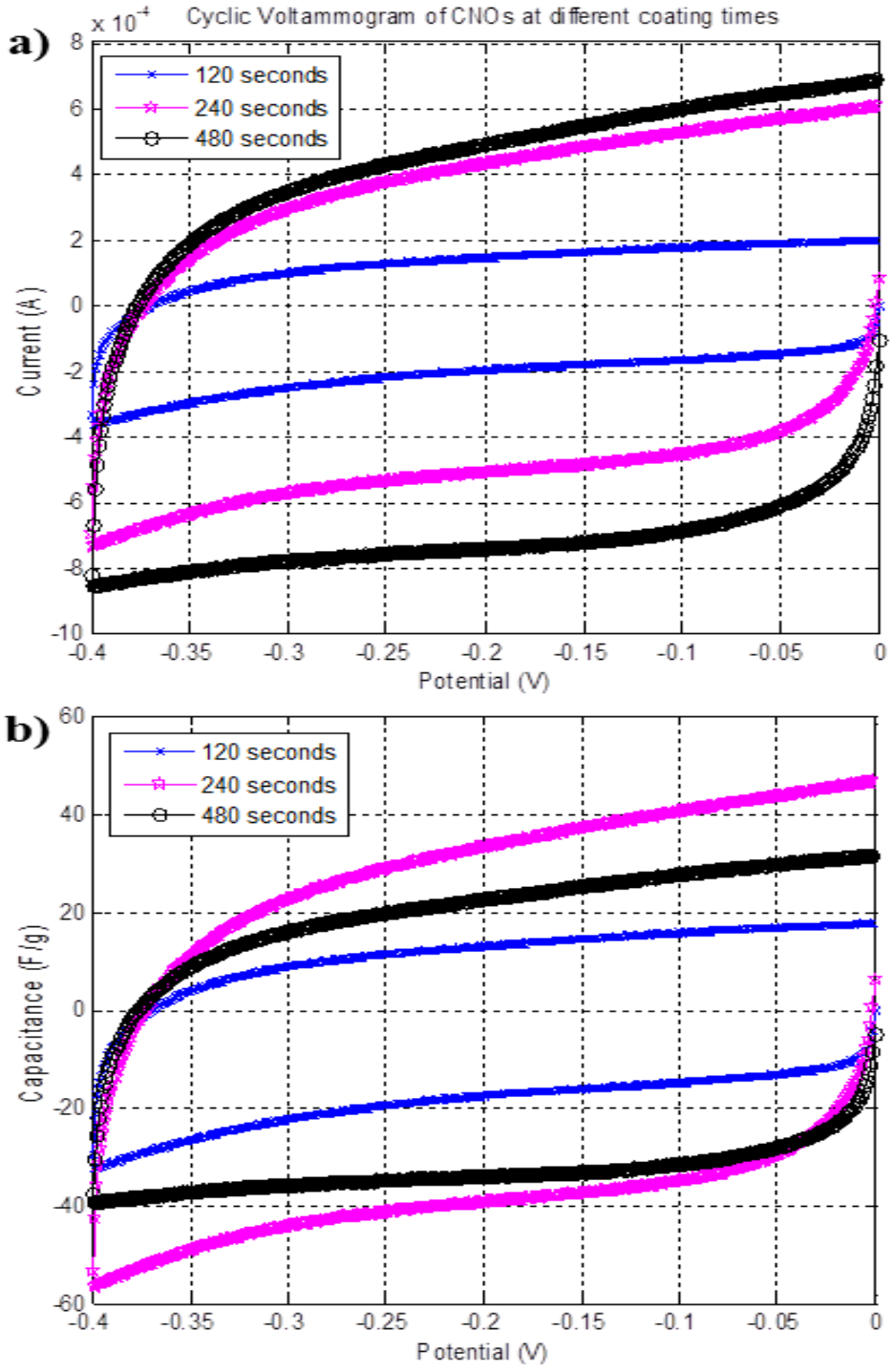

Figure 4.4. One cyclic voltammetry of CNO measured using a three-electrode configuration in 1 mol/l KNO_3. a) CV curves; b) specific capacitance for the three coating times.

Table 4.1 Specific energy, power and capacitance of different electrode materials in aqueous and nonaqueous electrolytes. a) Pure CNTs-based ultracapacitor, b) values obtained by effects of heating, c) values obtained by effects of the addition of functional groups (the groups of atoms that feature the chemical reactions of those molecules) onto the material's surface [16], d) values obtained by the combination of polymer and CNTs into a hybrid composite, and e) micrometer-sized supercapacitors.

	Aqueous-Inorganic Electrolyte (Decomposition voltage window 1 V)		
	Specific Energy	**Specific Power**	**Specific Capacitance**
	Wh/kg	**kW/kg**	**F/g**
CNT[17]a	0.5	-	102
CNT[18]b	-	20	180
CNT[19]c	0.92	4.8	350
CNT[20]d	228	2.25	485
CNO[21]c	8.5	153	111
CNO	5.6	2.5	40

	Nonaqueous-Organic Electrolyte (Decomposition voltage window 2.7 V)		
	Specific Energy	**Specific Power**	**Specific Capacitance**
	Wh/kg	**kW/kg**	**F/g**
Activated Carbon[22]	5-7	1-3	100
Activated Carbon[23]	6	5.9	94

Activated CNO UCs present higher performances than regular activated carbon UC. Even though, it should be stated the data presented in tale 4.1 are for two different electrolytes, aqueous-inorganic electrolyte and nonaqueous-organic electrolyte, respectively with 1 V and 2.7 V voltage windows.

4.5 Annealing

A variety of temperature treatment studies have been done, and it has been concluded that heat treatment positively affects the CNO properties. Fig. 4.5 shows the

high frequency impedance spectra of the CNO UC treated at different temperatures under a nitrogen environment for 1 hour versus untreated CNOs. The equivalent series resistance (ESR) reduction due to the heat treatment should lead to an increased power density. The power density enhancement by heat treatment of single-walled CNOs has been observed previously [2]).

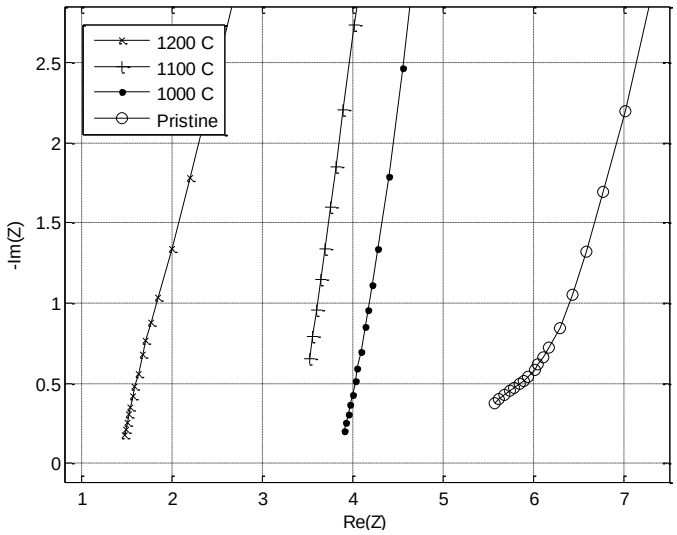

Figure 4.5. Annealing benefit for CNOs.

Literature

[1] Y. S. Zhou, W. Xiong, J. Park, M. Qian, M. Mahjouri-Samani, Y. Gao, L. Jiang, and Y. Lu, "Laser-Assisted Nanofabrication of Carbon Nanostructures," J. Laser Appl., vol. 24, no. 4, July 2012.

[2] H. Pan, J. Li, and Y. P. Feng, "Carbon Nanotubes for Supercapacitor," Nanoscale Research Letters, vol. 5, 2010, pp. 654–668, DOI 10.1007/s11671-009-9508-2.

[3] C. S. Du and N. Pan, "High Power Density Supercapacitor Electrodes of Carbon Nanotube Films by Electrophoretic Deposition," Nanotechnology, vol. 17, 2006, pp. 5314-5318.

[4] A. S. Sarac, M. Ates, and B. Kilic, "Electrochemical Impedance Spectroscopic Study of Polyaniline on Platinum, Glassy Carbon and Carbon Fiber Microelectrodes," Int. J. Electrochem. Sci., vol. 3, 2008, pp. 777-786.

[5] I. Streeter, G. G. Wildgoose, L. Shao, and R. G. Compton, "Cyclic Voltammetry on Electrode Surfaces Covered with Porous Layers: An Analysis of Electron Transfer Kinetics at Single-Walled Carbon Nanotube Modified Electrodes," J. Sensors and Actuators B: Chemical, vol. 133, issue 2, August 12, 2008, pp. 462-466.

[6] J. M. Miller, “Ultracapacitor Application,” IET Power and Energy Series, vol. 59, 2011.

[7] J. Lario-Garcıa and R. Pallas-Areny, “Constant-Phase Element Identification in Conductivity Sensors Using a Single Square Wave,” Sensors and Actuators, vol. 132, 2006, pp. 122-128.

[8] J. Ross Macdonald, “Impedance Spectroscopy,” Annals of Biomedical Engineering, vol. 20, 1992, pp. 289-305.

[9] S. H. Kim, W. Choi, K. B. B. Lee, and S. W. Choi, “Advanced Dynamic Simulation of Supercapacitors Considering Parameter Variation and Self-Discharge,” IEEE Transaction on Power Electronics, vol. 26, issue 11, 2011.

[10] F. Parigi, Y. Gao, T. Gachovska, J. L. Hudgins, D. Patterson, and Y. Lu, “Impedance-Based Simulation Model of Carbon Nano-Onions Ultracapacitors for e-Bike with Compact Energy Storage System,” 2012 IEEE Vehicle Power and Propulsion Conference, Oct. 9-12, 2012, Seoul, South Korea.

[11] S. H. Kim, W. Choi, K. B. B. Lee, and S. W. Choi, “Advanced Dynamic Simulation of Supercapacitors Considering Parameter Variation and Self-Discharge,” IEEE Transaction on Power Electronics, vol. 26, issue 11, 2011.

[12] J. Valsa and J. Vlach, “RC Models of a Constant Phase Element,” Int. J. Circ. Theor. Appl., vol. 41, 2013, pp. 59-67.

[13] D. Pech, M. Brunet, H. Durou, P. Huang, V. Mochalin, Y. Gogotsi, P.L. Taberna, and P. Simon, “Ultrahigh-Power Micrometre-Sized Supercapacitors Based on Onion-Like Carbon,” Nature Nanotechnology, vol. 5, July 2010, pp. 651-654.

[14] M. M. Shaijumon, F. S. Ou, L. Ci, and P. M. Ajayan, "Synthesis of Hybrid Nanowire Arrays and their Application as High Power Supercapacitor Electrodes," Chem. Commun., vol. 20, 2008, pp. 2373.

[15] D. Pech, M. Brunet, H. Durou, P. Huang, V. Mochalin, Y. Gogotsi, P.L. Taberna, and P. Simon, "Ultrahigh-Power Micrometre-Sized Supercapacitors Based on Onion-Like Carbon," Supplementary Information, Nature Nanotechnology, 2010, DOI: 10.1038/NNANO.2010.162.

[16] J. March, Advanced Organic Chemistry: Reactions, Mechanisms, and Structure (3rd ed.), New York: Wiley, ISBN 0-471-85472-7 (1985).

[17] C. Niu, E. K. Sichel, R. Hoch, D. Moy, and H. Tennent, "High Power Electrochemical Capacitors Based on Carbon Nanotube Electrodes," Applied Physics Letters, vol. 70, 1997, pp. 1480.

[18] K. H. An, W. S. Kim, Y. S. Park, Y. C. Choi, S. M. Lee, D. C. Chung, D. J. Bae, and S. C. Lim, "Supercapacitors Using Single-Walled Carbon Nanotube Electrodes," Adv. Mater, vol. 13, 2001, pp. 497.

[19] C. Zhou, S. Kumar, C. D. Doyle, and J. M. Tour, "Functionalized Single Wall Carbon Nanotubes Treated with Pyrrole for Electrochemical Supercapacitor Membranes," Chemistry of Materials, vol. 17, 2005, pp. 1997-2002.

[20] Y. K. Zhou, B. L. He, W. J. Zhou, and H. L. Li, “Enhanced Electrochemical Properties of Polyaniline-Coated Multiwall Carbon Nanotubes,” J. Electrochem. Soc., vol. 151, 2004, pp. A1052.

[21] Y. Gao, Y. S. Zhou, M. Qian, X. N. He, J. Redepenning, P. Goodman, H. M. Li, L. Jiang, and Y. F. Lu, “Chemical Activation of Carbon Nano-Onions for High-Rate Supercapacitor Electrodes,” Carbon, vol. 51, January 2013, pp. 52-58.

[22] A. Burke, “Ultracapacitor Technologies and Application in Hybrid and Electric Vehicles,” Int. J. Energy Res., vol. 34, 2010, pp. 133–151, doi: 10.1002/er.1654.

[23] Maxwell® Technologies, Datasheet K2 Series Ultracapacitors, Document Number: 1015370.3

CHAPTER 5. MODELING A CNO ULTRACAPACITOR

The schematic of the proposed ultracapacitor equivalent circuit is depicted in Figure 5.1. The CNO UC model is composed of three main sections that account for: parasitic internal inductance and resistance (L and R_e, respectively), energy storage (C_{dl}), and leakage resistance (R_c) coupled with a constant phase element, CPE.

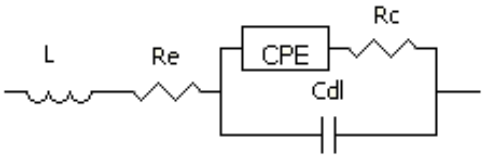

Figure 5.1. Proposed ultracapacitor equivalent circuit model.

A parasitic inductance, L, will always be part of any packaged device due to the path for current flow. A nonzero value is necessary to accurately describe the physical behavior of the UC at mid- and higher frequencies of operation. Incorrect use of this term has a significant effect on the estimations of R_e. Miller [1] found that the order of magnitude of L for activated carbon ultracapacitors is 20 nH, so this value was used as the initial value for the optimization process developed in this work.

5.1. Constant Phase Element

The CPE impedance is calculated by Eq. (5.1); it has two independent parameters: a real constant, Q, and a real exponent, β, where β is in the range of 0 to 1[1].

$$Z_Q = \frac{1}{Qs^{\beta}} \tag{5.1}$$

$s = j\omega$ is the angular frequency. For $\beta = 0$, Q has conductance behavior; for $\beta = 1$, Q is an ideal capacitor. Otherwise, the dimension of Q is $\sec^{\beta}/\Omega$.

At an angular frequency, $\omega = 1$ rad/s (0.159 Hz) the impedance magnitude of the CPE is $|Z| = 1/Q$. From the experimental impedance data, at $\omega = 1$ Q is 0.0064 $\sec^{\beta}/\Omega$.

To calculate the constant β, a plot of the imaginary part of the impedance as a function of frequency on a log-log scale is used. Fig. 5.2 shows the imaginary part of the measured impedance as the function of frequency and indicates an almost linear behavior (nearly constant β). Therefore, by using the data, the slope of the line gives the value of $\beta \approx 0.8$.

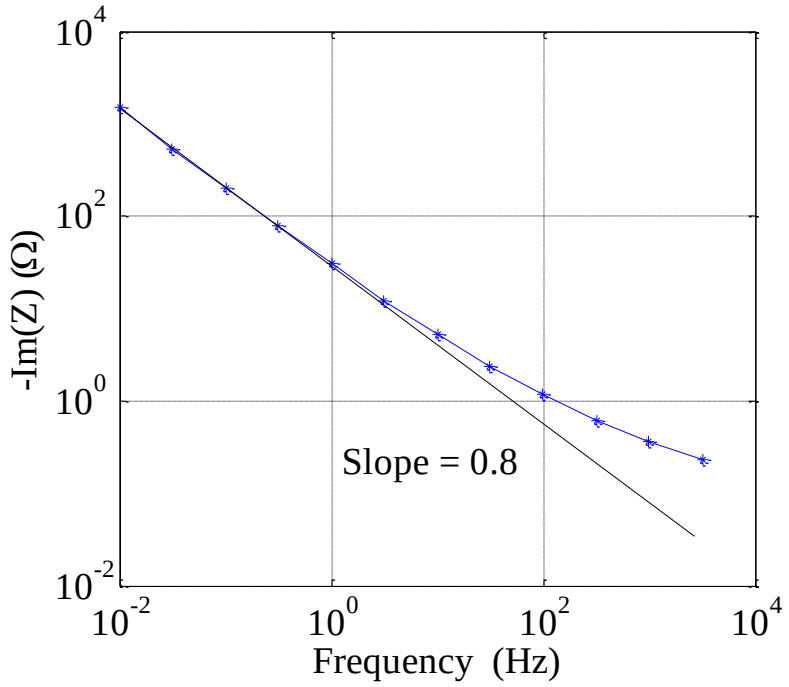

Figure 5.2. Imaginary part of the impedance as a function of frequency.

The CPE impedance could be calculated following another approach as indicated in Eq. (5.2) [1]. The CPE impedance, expressed in Eq. (5.2) has two independent parameters, α and the exponent β ($0 \leq \beta \leq 1$) of the angular frequency ($j\omega$). When $\beta = 1$, α, a derived term, has the dimensions admittance. When $\beta = 0$, α has a resistance behavior; otherwise it has units of Ω/sec^{β}.

$$Z_Q = \frac{\alpha}{s^{\beta}} \tag{5.2}$$

When $\beta = 0.5$, it is also referred to as Warburg impedance, $Z_Q = Z_W$. Eq. (5.2) has been shown to be described with α as given by Eq. (5.3) for this specific value of β.

$$\alpha = \frac{RT}{\sqrt{2}n^2FA}\left(\frac{2\,10^3}{C_0\sqrt{D_c}}\right) \tag{5.3}$$

where R represents the gas law constant 9.314 J/Kmol; F is Faraday's constant of 96,485 C/mol, $n = 1$, the involved number of electron exchanges, $T = 298$ K as the absolute temperature, A (cm^2) is the electrode area, $C_0 = 1$ mol/L, the electrolyte concentration, and D_C the ion diffusion constant.

The impedance function of the equivalent circuit in Fig. 5.1, $Z(\omega)$, can be written as Eq. (5.4).

$$Z(\omega) = Z'(\omega) - jZ''(\omega) \tag{5.4}$$

For the circuit in Fig. 5.1, Z' and Z'' are:

$$Z' = R_e + \left[\frac{\frac{R_C}{\omega^2 C_1^2} + \frac{\alpha\omega^{-(\beta+2)}}{C_1^2}\cos\left(\frac{\pi\beta}{2}\right)}{R_C^2 + \frac{1}{\omega^2 C_1^2} + \alpha^2\omega^{2\beta} + 2\alpha\omega^{-\beta}\left(R_C\cos\left(\frac{\pi\beta}{2}\right) + \frac{1}{\omega C_1}\sin\left(\frac{\pi\beta}{2}\right)\right)}\right] \tag{5.5}$$

$$Z'' = -\frac{\left[\frac{R_C^2}{\omega C_1} + \frac{\alpha^2\omega^{-(2\beta+1)}}{C_1} + \frac{2\alpha R_C\omega^{-(\beta+1)}}{C_1}\cos\left(\frac{\pi\beta}{2}\right) + \frac{\alpha\omega^{-(\beta+2)}}{C_1^2}\sin\left(\frac{\pi\beta}{2}\right)\right]}{\left[R_C^2 + \frac{1}{\omega^2 C_1^2} + \alpha^2\omega^{-2\beta} + 2\alpha R_C\omega^{-\beta}\cos\left(\frac{\pi\beta}{2}\right) + \frac{2\alpha}{C_1}\omega^{-(\beta+1)}\sin\left(\frac{\pi\beta}{2}\right)\right]} \tag{5.6}$$

To find the magnitude of α, use (5.3) to match the Nyquist frequency response to the analytically derived impedance function (5.4) with the values presented above and mentioned in (5.3).

The diffusion constant D_c is found by iteration of (5.2), (5.3), and the ultracapacitor cell parameters. With D_c known, the value of α can be determined.

Figure 5.3 shows the two-dimensional normalized squared error in the impedance function, (5.2), based on variation of β and D_c. The red square box at the bottom of the Fig. 5.3 indicates the minimum error for $\beta = 0.825$ and $Dc = 1 \cdot 10^{-5}$. In conclusion, we can state that both methods for estimating β gave comparable values, hence there is confidence in the value extrapolated for use in the new UC model.

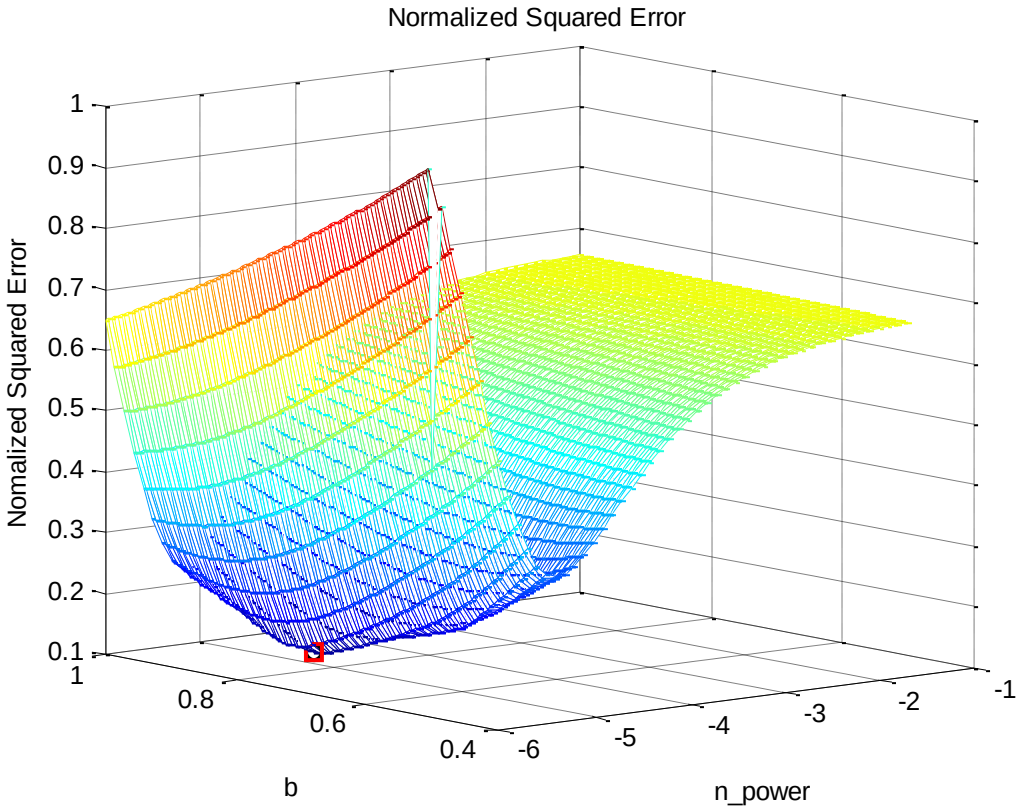

Figure 5.3. Normalized Squared Error in the impedance function with variations in β and D_c.

5.2 CPE Model

To be able to use the CNO UC model in circuit simulation/design software, it is desirable to model the CPE with circuit elements as well. The CPE has previously been modeled as a ladder network with RC components [2]. As a reminder, a CPE is an

element with a constant phase shift over a given frequency band. The inputs of the design model procedure that interest us here are the fractional capacitor exponent β, used to match the impedance spectra in the low frequency zone of the Nyquist plot at which the phase angle is nearly constant. Fig. 5.4 shows the schematic of the CPE equivalent circuit used in this study. The desired frequency bandwidth dictates the number of branches (larger bandwidth requires more branches). The RC parameters, with R_1 and C_1 given, have recursive values, defined by (5.7) [3]:

$$R_{k+1} = aR_k, \quad C_{k+1} = bC_k, \quad k = 1, \dots, m-1 \quad 0 < a < 1, \quad 0 < b < 1 \tag{5.7}$$

The average phase angle in degrees is defined by (5.8):

$$\varphi = 90 \, \frac{log\, a}{log(ab)} \tag{5.8}$$

The phase ripple amplitude, $\Delta\varphi$, is related to parameters *a* and *b* by (5.9):

$$ab = \frac{0.24}{1+ \Delta\varphi} \tag{5.9}$$

Therefore, the phase angle and its ripple define parameters *a* and *b* directly.

The bandwidth is bounded by ω_{min} and ω_{max} (5.10):

$$\omega_{min} \approx \frac{1}{R_1 C_1}, \; \omega_{max} \approx \frac{\omega_{min}}{(ab)^{m-1}}. \tag{5.10}$$

where, *m* the number of branches, is determined by solving (5.10) .

$$m = 1 - \frac{log\left(\frac{\omega_{max}}{\omega_{min}}\right)}{log(ab)} \tag{5.11}$$

In addition, the correction elements, R_p and C_p, due to the limited number of branches, are determined by (5.12):

$$C_p = \frac{C_1 b^m}{1-b}, \; R_p = R_1 \frac{1-a}{a}. \tag{5.12}$$

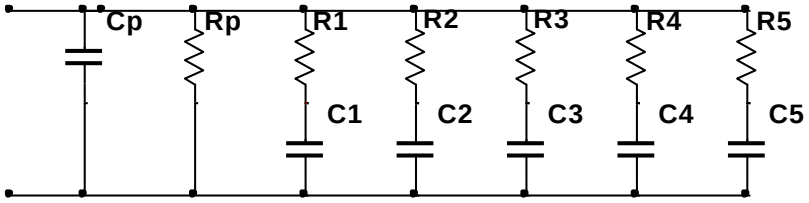

Figure 5.4. CPE equivalent circuit model.

In designing the CPE, the value of φ, given in (5.8), and the tolerable ripple, Δφ, in the phase are chosen. From these values and the chosen bandwidth, parameters *a* and *b* can be found.

The experimental values of the CNO electrode can be extracted to give R_e = 1.96 Ω, R_c = 2.27 Ω, and C_{dl} = 0.5 mF. Initial values of the ladder network approximation for the CPE are chosen and, alongside the other equivalent circuit values extracted, are inserted into the model; and a simulation of operational behavior is performed using ZView™. This software is often used in electrochemical systems to minimize chi-squared and sum of square errors, and it is used in this study to optimize the parameters of the CNO model. The optimized parameters of the CPE are presented in Table 5.1.

The complete equivalent circuit model of a CNO UC with extracted parameter values and optimized values for the CPE equivalent is shown in Figure 5.5. The experimental and simulated data, one on top of the other, are shown in Figure 5.6.

Table 5.1. CPE equivalent circuit model with optimized parameter values.

K	P	1	2	3	4	5
C [mF]	2.5	100	2.79	2.92	33.6	2
R [Ω]	7.6e8	99378	2096	18.42	17030	427

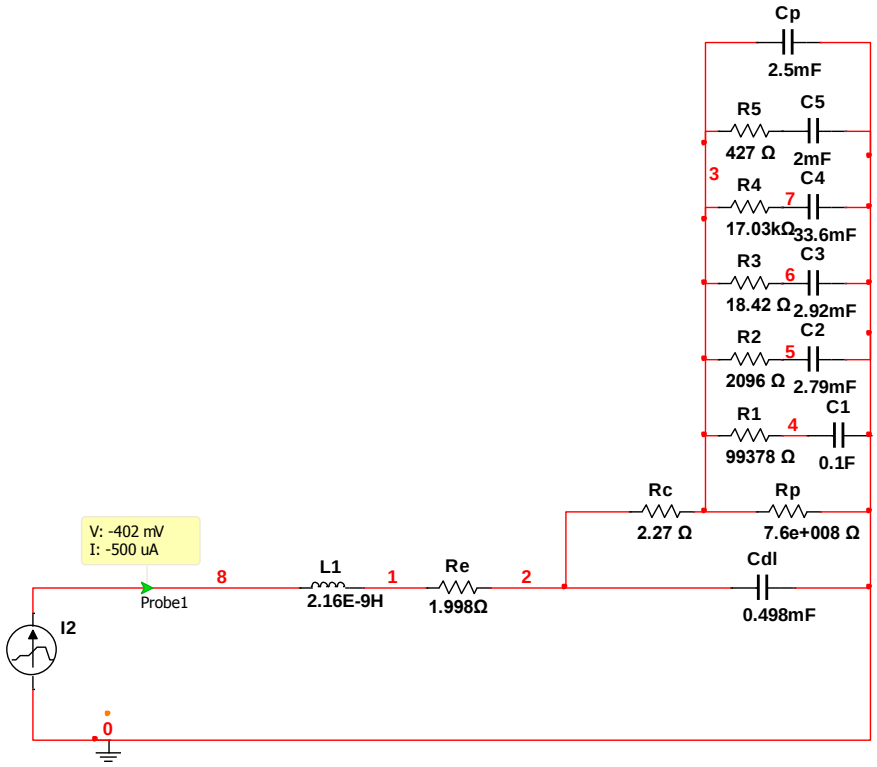

Figure 5.5. Equivalent circuit model of a CNO ultracapacitor.

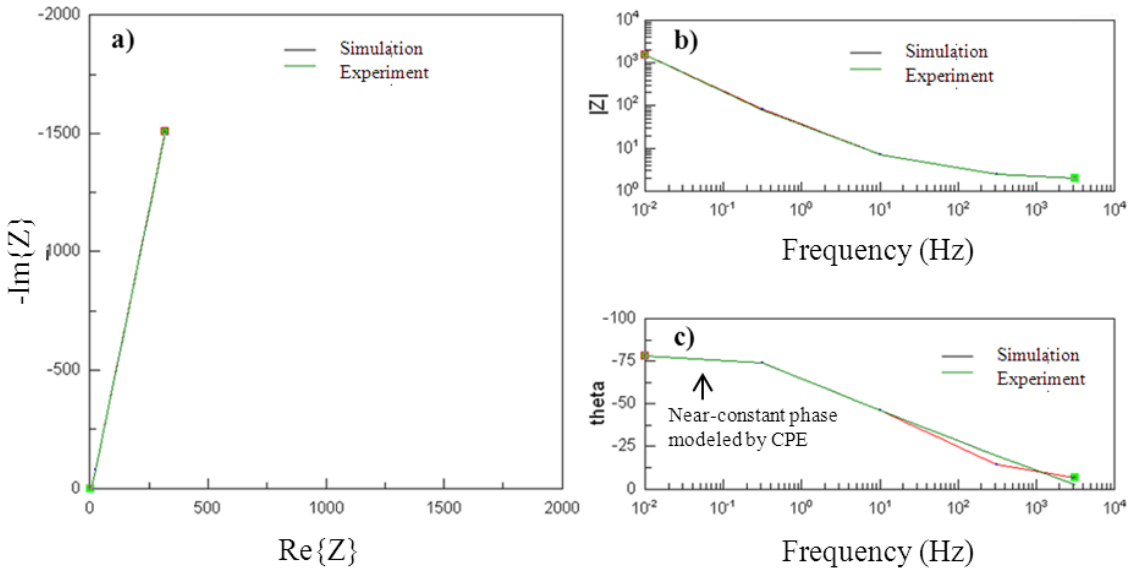

Figure 5.6. Measured and simulated data obtained by the CNO model shown in Fig. 5.5; a) complex plane representation of measured and calculated impedance spectra, b) impedance magnitude vs. frequency, and c) phase angle vs. frequency.

During the experiment, 12 frequency points (independent values), representing all of the spectra, were investigated. All measurements between the minimum and maximum frequency fit the curve well. The chi-square test was used to determine the goodness of the fit between the equivalent circuit model simulation data (theoretical data) and experimental data. Therefore, according to the chi-square theory [2], there are 11 degrees of freedom, giving a critical value of 19.675 with a percentile of 5%. The results give a value of 0.01 and are, therefore, consistent with the experimental results to within a 95% chance of probability. Fig. 5.7 shows the equivalent model verification for a standard applied test excitation. It can be seen that the UC model developed in this work fits exceedingly well with the experimental results for the applied excitation.

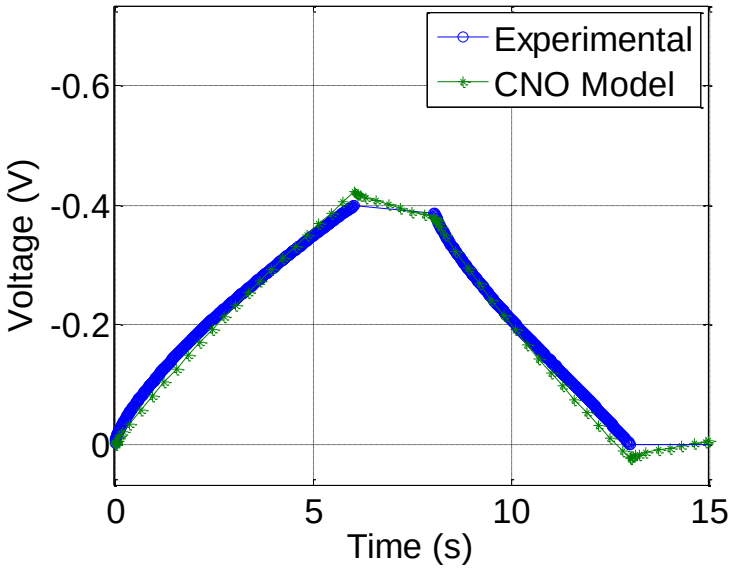

Figure 5.7. Experimental results compared to the model equivalent circuit simulation of the voltage response to an applied standard test current excitation.

5.3 CNO UC Model vs. Canonical models

The CNO UC model is compared with two different equivalent circuits developed by other investigators. The UC simple model, often used for first estimates in ultracapacitor studies [4], is shown in Fig. 5.8a. A Randles equivalent circuit with a Warburg element, often used to model the interfacial electrochemical reactions of flat electrodes [5], is shown in Fig. 5.8b. The equivalent circuit parameters for these two circuits specifically using the CNO UC experimental data has been determined by ZSimDemo 3.30d software. Fig. 5.9 shows the impedance magnitude comparing the three models under investigation with the experimental data as a function of frequency. and Fig. 5.10 shows the phase angle of the three models under investigation and the experimental data in the function of frequency.

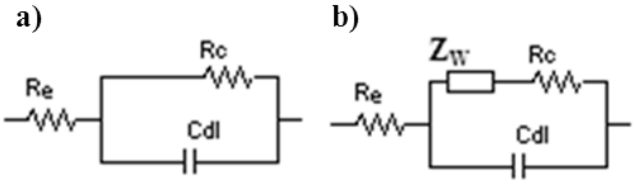

Figure 5.8. a) Simple model: R_e = 2.8 Ω, R_c = 5260 Ω, C_{dl} = 0.00435 F, b) Warburg equivalent circuit: R_e = 2.6 Ω, Z_W = 0.002313 S·sec$^{1/2}$, R_c = 2.8 Ω, C_{dl} = 0.0031 F.

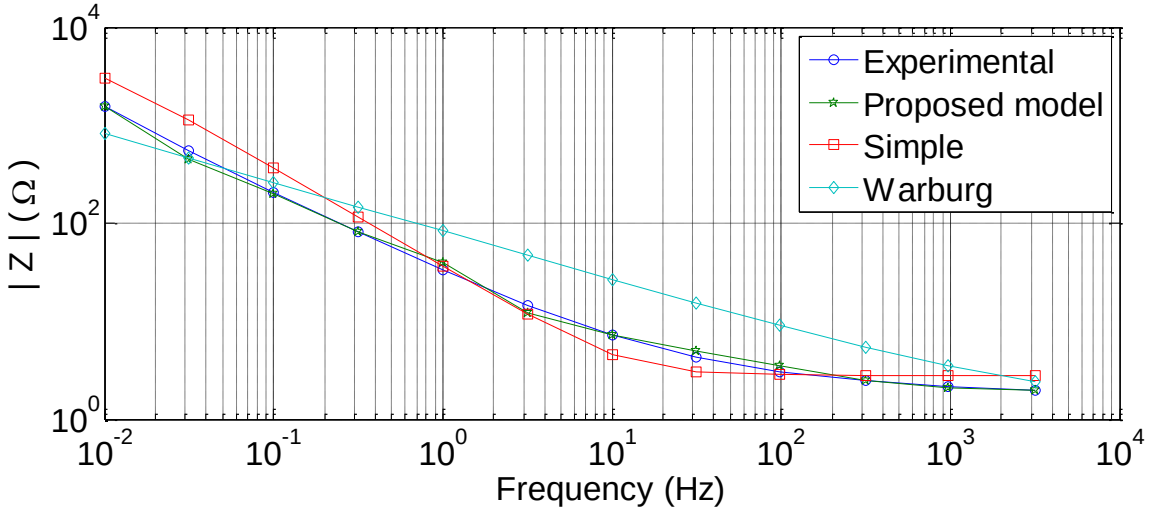

Figure 5.9. Impedance magnitude of the three models under investigation compared to each other and the experimental data as a function of frequency.

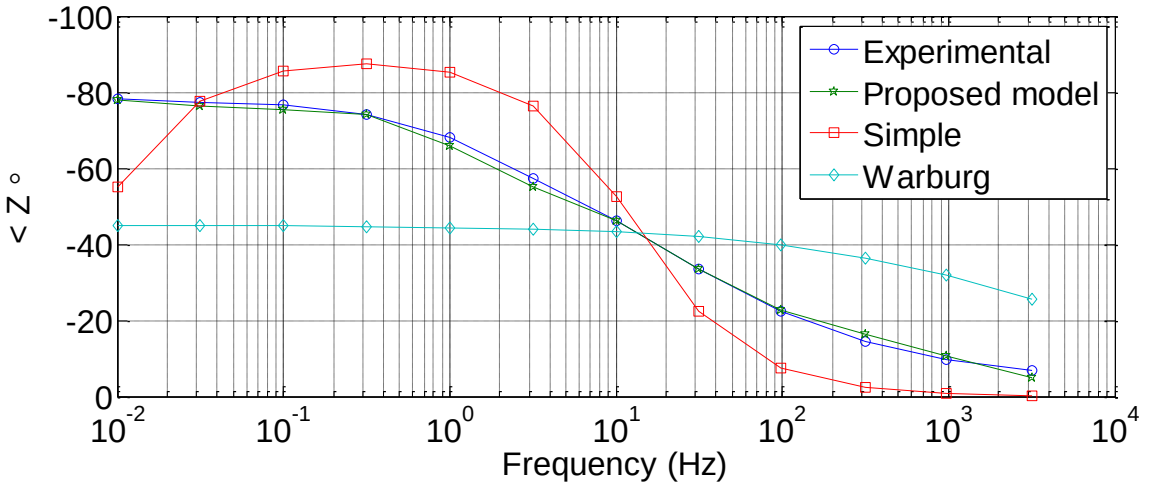

Figure 5.10. Phase angle of the three models under investigation compared to each other and the experimental data as a function of frequency.

From Fig. 5.9, it can be seen that at the resonant frequency, 3.17 kHz (the frequency at which the impedance spectra cross the real axis in the Nyquist plot in Fig. 4.3), the three models match the experimental impedance data fairly well. The phase angle shows a 45° slope at low frequency, which is typical of a so-called Warburg

impedance [5]. At low frequency, the simple model and the Warburg model deviate substantially from the experimental data and the newly proposed model. The proposed model fits the experimental data quite well along all the frequencies of interest. Based on the comparison, the other two models are less accurate then the proposed model.

Literature

[1] J. M. Miller, "Ultracapacitor Application," IET Power and Energy Series, vol. 59, 2011.

[2] D. E. Hinkle, W. Wiersma, and S. G. Jurs, Applied Statistics for the Behavioral Sciences, 5th Ed., Boston, MA: Houghton Mifflin, 2003.

[3] J. Valsa and J. Vlach, "RC Models of a Constant Phase Element," Int. J. Circ. Theor. Appl., vol. 41, 2013, pp. 59-67.

[4] R. L. Spyker and R. M. Nelms, "Classical Equivalent Circuit Parameters for a Double-Layer Capacitor," IEEE Transactions on Aerospace and Electronic Systems, vol. 36, issue 3, July 2000, pp. 829-836.

[5] S. Buller, E. Karden, D. Kok, and R. W. De Doncker, "Modeling the Dynamic Behavior of Supercapacitors Using Impedance Spectroscopy," IEEE Transactions on Industry Applications, vol. 38, issue 6, 2002, pp. 1622-1626.

CHAPTER 6. SUMMARY AND CONTINUING WORK

This paper describes a novel ultracapacitor made from carbon nano-onions. The CNO electrodes were characterized by electrochemical impedance spectroscopy and cyclic voltammetry. A new CNO ultracapacitor model composed of an LRC and a constant phase element was developed and verified through experiments and simulations. This model, thanks to the high ductility of the constant phase element construction, fits the data better in the low frequency region than the other models considered. The constant phase element capability of tuning the frequency range at which the phase angle stays constant makes this model powerful for CNO material and makes it possible to match the points for a wider frequency window.

The parameter extraction procedure for the proposed model is straightforward using standard electrochemical measurement techniques. The chi-square test was used to determine the quality of the fit between the equivalent circuit model simulation data (theoretical data) and experimental data, using ZView^{TM} software. During the experiment, 12 frequency points (independent values) were investigated. The results showed that the chi-square for the equivalent circuit model and the experimental data was 0.01. The simulations are, therefore, consistent with the experimental results to within a 95% probability. Also, the proposed model has been compared to a simple ultracapacitor model and a Warburg model. Based on the comparison, the other two models are less accurate than the proposed one.

Future work includes the scaling up of the cell size to reduce the equivalent series resistance and, therefore, to approach the real-life application where the ESR is on the

order of tenths of Ohms. Annealing the CNOs before assembling the UC results in the ESR decreasing. This work developed the processing techniques that consistently produce quality electrodes for UC applications. Further work is needed to scale up to a manufacturing level, but no technical barriers currently appear to limit this development.